Toxicology and Applied Pharmacology 256 (2011) 8–23

Contents lists available at ScienceDirect

Toxicology and Applied Pharmacology

journal homepage: www.elsevier.com/locate/ytaap

Involvement of phorbol-12-myristate-13-acetate-induced protein 1 in goniothalamin-induced TP53-dependent and -independent apoptosis in hepatocellular carcinoma-derived cells

Kung-Kai Kuo [a,b,1], Yi-Ling Chen [c,d,1], Lih-Ren Chen [d,e,1], Chien-Feng Li [c,f,g], Yu-Hsuan Lan [h], Fang-Rong Chang [i], Yang-Chang Wu [j], Yow-Ling Shiue [c,*]

[a] Department of Surgery, Chung-Ho Memorial Hospital, Kaohsiung Medical University, Kaohsiung, Taiwan
[b] Cancer Center, Kaohsiung Medical University Hospital, Kaohsiung, Taiwan
[c] Institute of Biomedical Science, National Sun Yat-sen University, Kaohsiung, Taiwan
[d] Division of Physiology, Livestock Research Institute, Council of Agriculture, Executive Yuan, Taiwan
[e] Institute of Biotechnology, Southern Taiwan University of Technology, Tainan, Taiwan
[f] Department of Pathology, Chi-Mei Foundation Medical Center, Tainan, Taiwan
[g] National Institute of Cancer Research, National Health Research Institutes, Tainan, Taiwan
[h] School of Pharmacy, China Medical University, Taichung, Taiwan
[i] Graduate Institute of Natural Products, Kaohsiung Medical University, Kaohsiung, Taiwan
[j] Graduate Institute of Integrated Medicine, College of Chinese Medicine, China Medical University, Taichung, Taiwan

ARTICLE INFO

Article history:
Received 29 April 2011
Revised 3 July 2011
Accepted 6 July 2011
Available online 19 July 2011

Keywords:
Apoptosis
Goniothalamin (GTN)
Hep-3B
Phorbol-12-myristate-13-acetate-induced protein 1 (PMAIP1)
SK-Hep1
Tumor protein p53 (TP53)

ABSTRACT

The objective was to investigate the upstream apoptotic mechanisms that were triggered by a styrylpyrone derivative, goniothalamin (GTN), in tumor protein p53 (TP53)-positive and -negative hepatocellular carcinoma (HCC)-derived cells. Effects of GTN were evaluated by the flow cytometry, alkaline comet assay, immunocytochemistry, small-hairpin RNA interference, mitochondria/cytosol fractionation, quantitative reverse transcription-polymerase chain reaction, immunoblotting analysis and caspase 3 activity assays in two HCC-derived cell lines. Results indicated that GTN triggered phorbol-12-myristate-13-acetate-induced protein 1 (*PMAIP1*, also known as *NOXA*)-mediated apoptosis via TP53-dependent and -independent pathways. In TP53-positive SK-Hep1 cells, GTN furthermore induced TP53 transcription-dependent and -independent apoptosis. After GTN treatment, accumulation of reactive oxygen species, formation of DNA double-strand breaks, transactivation of *TP53* and/or *PMAIP1* gene, translocation of TP53 and/or PMAIP1 proteins to mitochondria, release of cytochrome *c* from mitochondria, cleavage of caspases and induction of apoptosis in both cell lines were sustained. GTN might represent a novel class of anticancer drug that induces apoptosis in HCC-derived cells through *PMAIP1* transactivation regardless of the status of *TP53* gene.

Introduction

Studies performed over the past two decades by us and other researchers have shown that, goniothalamin (GTN), a natural compound, is cytotoxic to a variety of tumor cell lines including those from the breast, blood, ovary, lung, kidney, prostate, hepatoblast, and colon (Fatima et al., 2006; Inayat-Hussain et al., 1999; Inayat-Hussain et al., 2003; Inayat-Hussain et al., 2010; Lan et al., 2003; Lan et al., 2005; Lan et al., 2006; Wu et al., 1991; Zhou et al., 2005). Besides, GTN is more cytotoxic to cancer cells than to normal cells (Wattanapiromsakul et al., 2005). In Jurkat T-lymphocytes and HL-60 leukemia cells, mitochondria and caspases (CASPs) are evidently involved in GTN-induced apoptosis (Inayat-Hussain et al., 1999; Inayat-Hussain et al., 2003; Inayat-Hussain et al., 2010). However, the mechanism of GTN-induced apoptosis upstream of the mitochondria is not clearly understood, except for DNA damage and apoptosis via oxidative stress. Recently, GTN-induced apoptosis of Jurkat T-lymphocytes through the CASP2- and B-cell leukemia/lymphoma 2 (BCL2)-independent pathways has been described (Inayat-Hussain et al., 2010).

Hepatocellular carcinoma (HCC) is the most common primary malignant neoplasm of the liver worldwide, accounting for approximately 6% of all human cancers annually (Nowak et al., 2004). Although substantial advances have been made in chemotherapy regimens for HCC, the efficacy of drugs is often hampered by a range of adverse side effects (Worns et al., 2009). Clinical and genetic heterogeneity observed in HCC patients further complicates the use

* Corresponding author at: Institute of Biomedical Science, National Sun Yat-sen University, 80424 Kaohsiung, Taiwan, Address: 70, Leinhai Rd. Kaohsiung, Taiwan. Fax: +886 7 525 0197.
E-mail address: ylshiue@mail.nsysu.edu.tw (Y.-L. Shiue).
[1] These authors contribute equally.

0041-008X/$ – see front matter © 2011 Elsevier Inc. All rights reserved.
doi:10.1016/j.taap.2011.07.002

of general therapies (Hoshida et al., 2010). Accordingly, it is essential to explore new approaches for the development of effective therapies against HCC. Insufficient apoptosis has been associated with the development and progression of HCCs. Therefore, modulation of apoptosis by targeting the components and regulators of the apoptotic machinery to restore apoptotic function or repress prosurvival signals is a rational approach for HCC treatment (Fabregat, 2009).

Apoptosis is regulated by adversarial interactions between BCL2 family proteins, including the antiapoptotic proteins, BCL2 itself, BCL2-related myeloid cell leukemia sequence 1 (MCL1), BLC2-associated X protein (BAX), and BCL2-antagonist/killer 1(BAK1) (Adams and Cory, 2007). These proteins have emerged as the major regulators of HCC apoptosis. Moreover, the proapoptotic BH3-only protein like BCL2 binding component 3 (BBC3, also known as PUMA), phorbol-12-myristate-13-acetate-induced protein 1 (PMAIP1, also known as NOXA) and BCL2-like 11 (BCL2L11, also known as BIM) play key roles in coupling the specific death stimuli to the core apoptotic machinery. The direct activation model of apoptosis suggests that BH3-only proteins can either function as sensitizers or activators. This model postulates that activator BH3-only proteins are sequestered by binding to antiapoptotic proteins. Increase in the cellular levels of sensitizer proteins, including BBC3 and PMAIP1, results in the displacement of activator proteins such as BCL2L11. The displaced BCL2L11 then interacts with BAX or BAK1, resulting in change in their conformation and insertion into the outer mitochondrial membrane. The subsequent release of cytochrome *c*, somatic (CYCS) from the mitochondria activates the CASPs, which are required for the initiation of apoptosis (Ghiotto et al., 2010).

Therefore, the mitochondrion plays a critical role in apoptosis (Moll and Zaika, 2001). Tumor protein p53 (TP53) controls apoptosis, in part, via positive or negative transcriptional regulation of various BCL2 family proteins such as BCL2, BBC3, BAX and PMAIP1 (Yu and Zhang, 2005). In addition, two other members of the TP53 family, tumor protein 63 (TP63) and tumor protein (TP73) were classified in relation to TP53 based on their structural similarity (Kaghad et al., 1997; Yang et al., 1998). The TP63 and TP73 bound *PMAIP1* DNA probe after ionizing radiation or ultraviolet B treatment, correlating with *PMAIP1* mRNA induction and with cell cycle arrest and apoptosis (Kulesz-Martin et al., 2005).

TP53 can additionally induce apoptosis in a transcription-independent manner by directly targeting the mitochondria (Moll et al., 2005). It has been shown that TP53 translocates to the mitochondria within 1 h after γ-irradiation in various cancer cell lines. This translocation promotes changes in the mitochondrial membrane potential and subsequent release of CYCS (Marchenko et al., 2000). In contrast, TP53-independent apoptosis mediated by BBC3 in isogenic colon cancer cells (Watson et al., 2010) and PMAIP1 in chronic lymphocytic leukemia cells (Steele et al., 2009) have also been reported. In the present study, we evaluated the apoptotic effects of GTN on TP53-positive and TP53-negative HCC-derived cells. We

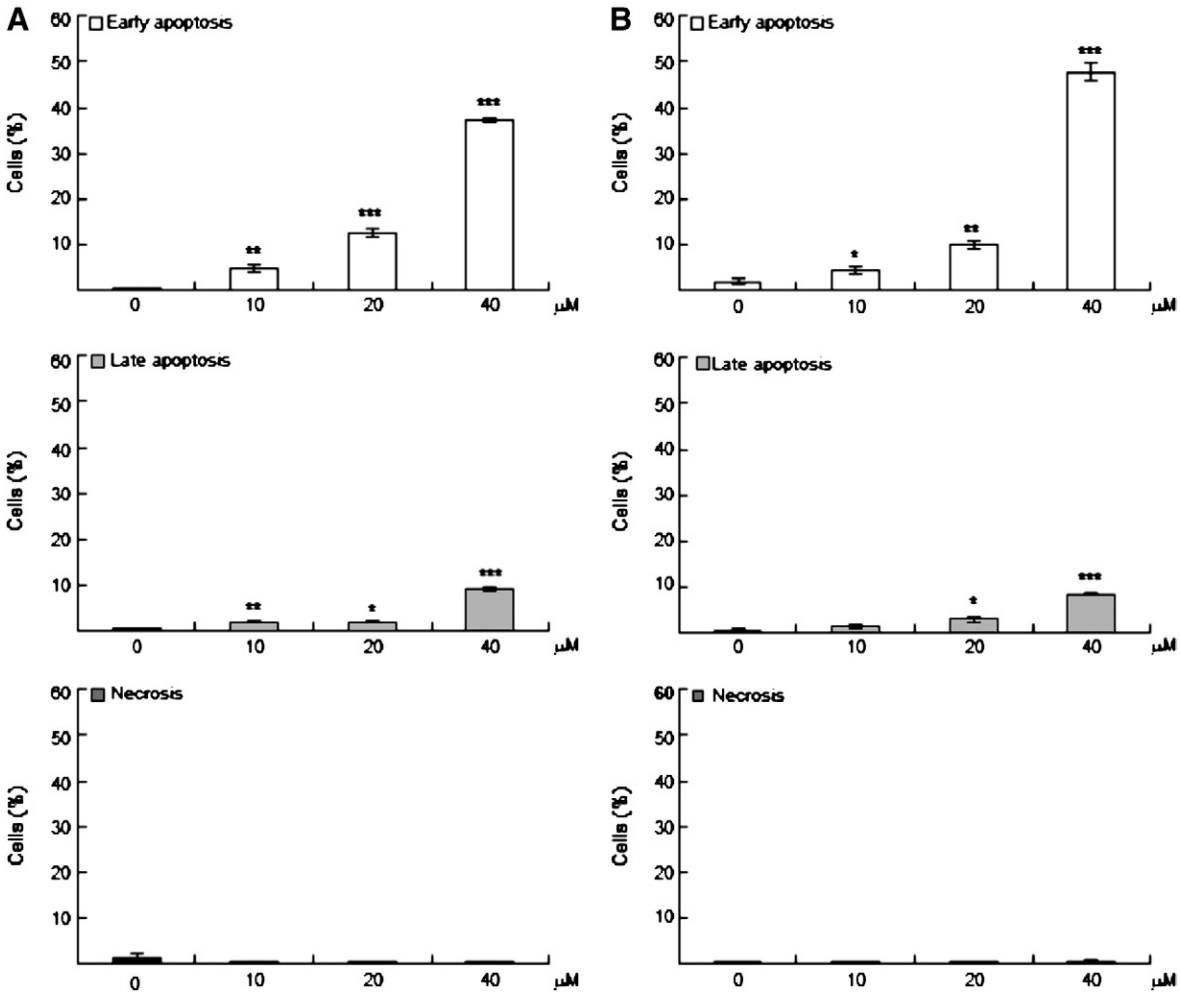

Fig. 1. GTN induced early and late apoptosis but not neurosis in TP53-positive SK-Hep1 (A), and TP53-negative Hep-3B (B) cells in a dose-dependent manner. Statistical significance between the treated group (10, 20 or 40 μM) and its corresponding control (0 μM): **P*<0.05; ***P*<0.01 and ****P*<0.001.

identified that GTN induces the accumulation of reactive oxygen species (ROS), causes DNA double-strand breaks, directs TP53-dependent and -independent *PMAIP1* transactivation, translocates TP53 and/or PMAIP1 proteins to the mitochondria, and finally initiates CASP-mediated apoptosis.

Materials and methods

Cell culture. Two HCC-derived cell lines, SK-Hep1 and Hep-3B, were maintained in a humidified incubator with 5% CO_2 atmosphere at 37 °C and supplemented with the following nutrients and antibiotics:

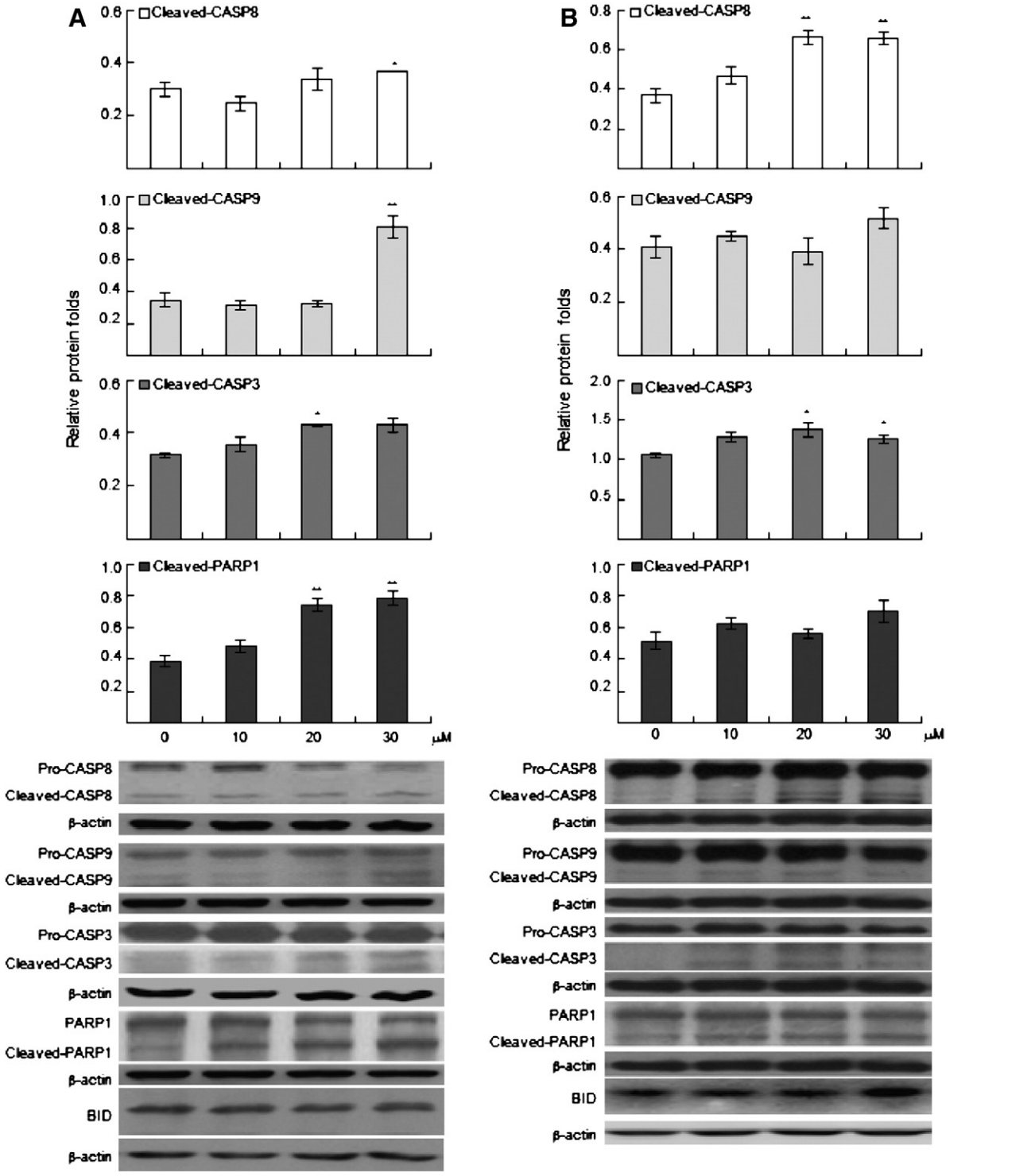

Fig. 2. GTN induced caspase-mediated apoptosis in TP53-positive SK-Hep1 and TP53-negative Hep-3B cells. GTN induced the cleavages of CASP8, CASP9, CASP3 and PARP1 proteins in SK-Hep1 cells (A), and the cleavages of CASP8 and CASP3 in Hep-3B cells (B) in a dose-dependent manner. Treatment with z-VAD-FMK alone suppressed endogenous and GTN-induced percentages of apoptotic cells (C, D); and CASP3 activities in SK-Hep1 (E) and Hep-3B (F) cells. Treatments with z-VAD-FMK decreased GTN-induced PARP1 protein cleavage in both cell lines (G, H). All experiments were triplicated and results are expressed as mean SEM. One representative image is shown for the immunoblotting analysis and -actin served as the loading control. Statistical significance: $^{*}P<0.05$; $^{**}P<0.01$ and $^{***}P<0.001$.

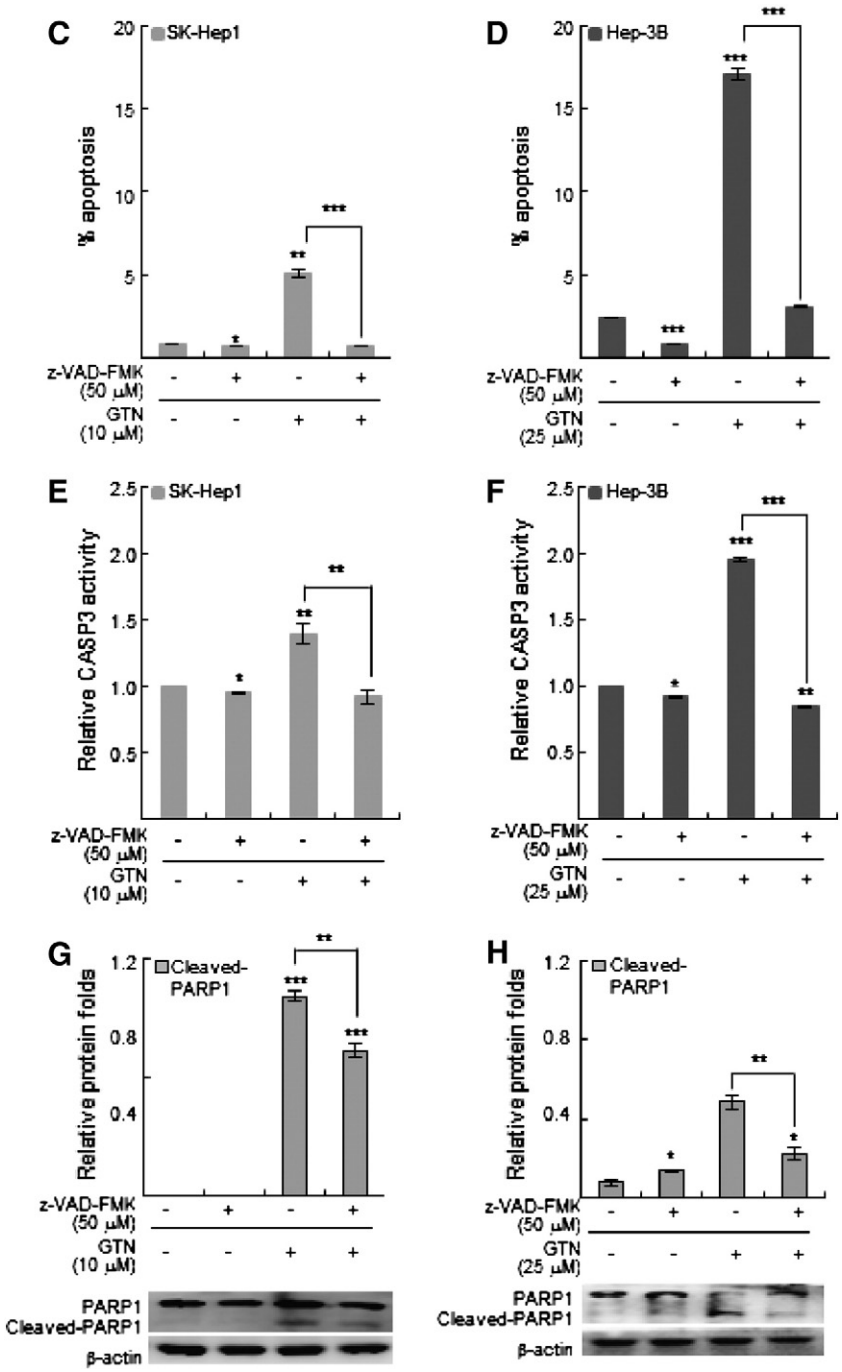

Fig. 2 (*continued*).

Dulbecco's Modified Eagle's Medium containing 10% fetal bovine serum, 1% L-glutamine (2 mM), 1% nonessential amino acids, 1 mM sodium pyruvate, 50 IU/mL penicillin, and 50 μg/mL streptomycin (Gibco Invitrogen Corporation, Carlsbad, CA, USA). These two cell lines were known to have distinctly different genetic backgrounds. The SK-Hep1 is characterized by expression of TP53, cyclin-dependent kinase inhibitor 1A (also known as $p21^{Cip1}$), retinoblastoma 1 proteins, and absence of hepatitis B virus protein, while pertinent features of these markers are completely opposite in Hep-3B cells (Bressac et al., 1990).

Chemicals. GTN (see Supplementary Fig. S1A in the online version of this article) was isolated from the leaves and stems of *Goniothalamus amuyon* in our previous study (Lan et al., 2005); dissolved in dimethyl sulfoxide (DMSO). The maximum amount of DMSO in culture medium was 1/1000. All chemicals unless otherwise stated were purchased from Sigma-Aldrich (St. Louis, MO, USA).

Apoptosis assays. Cells were plated at a cell density of 10^5 per 60 mm Petri dish for 24 h. Apoptosis was detected after GTN [0 (DMSO, control), 10, 20 or 40 μM] treatments for 24 h and quantified by phosphatidylserine exposure. After GTN treatment cells were centrifuged for 5 min at 700 × *g* and resuspended in Annexin V Binding Buffer (#BMS306F1, Bender MedSystems, Burlingame, CA, USA). Annexin V with fluorescein isothiocynate (FITC)-labeled nucleotides as well as propidium iodide (PI) staining was carried out following the manufacturer's instructions. Subsequent to an incubation of 10 min,

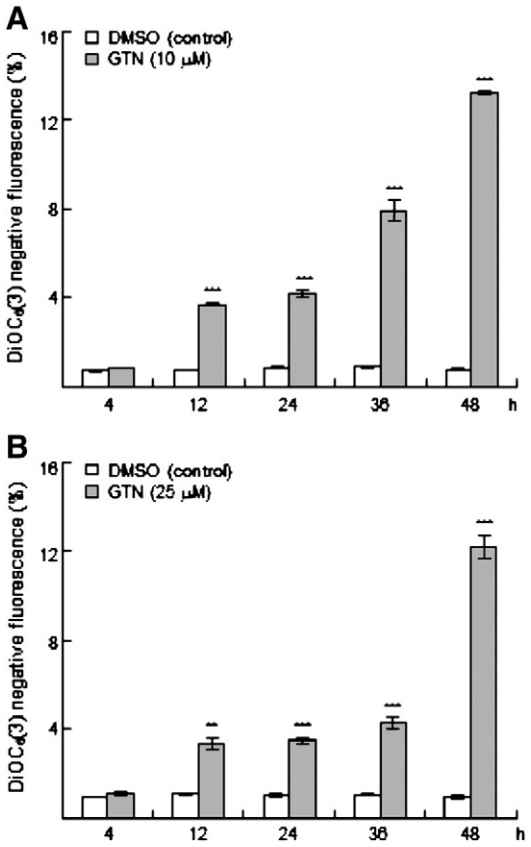

Fig. 3. GTN treatment for 12 to 48 h perturbed the mitochondrial membrane integrity in TP53-positive SK-Hep1 (A), and TP53-negative Hep-3B (B) cells. Cells were treated with 0 (DMSO, control), 10 (SK-Hep1) or 25 (Hep-3B) μM GTN for indicated time periods. Percentage of cells displaying negative $DiOC_6(3)$ fluorescence is shown in the y-axis. All experiments were triplicated and results are expressed as mean ± SEM. Statistical significance between the treated group and its corresponding control: $^{**}P<0.01$ and $^{***}P<0.001$.

the analysis was performed by using an IPICS® XL-MCL™ flow cytometer (Beckman Coulter, Fullerton, CA, USA). All experiments were triplicated and results are expressed as mean ± SEM.

CASP3 activity assay. The Caspase 3 Colorimetric Assay Kit (#1008-200, BioVision Inc., Mountain View, CA, USA) was used to determine the CASP3 activity, according to the standard procedure. A total of 10^6 cells were treated with carbobenzoxy-valyl-alanyl-aspartyl-(O-methyl)-fluoromethylketone (z-VAD-FMK; 50 μM) for 1 h or GTN for another 24 h, and then subjected to assay by spectrophotometry. Concisely, cells were centrifuged (700 × *g*, 4 °C) for 5 min and the pellet was resuspended in 50 μL of chilled Cell Lysis Buffer and incubated on ice for 30 min. The supernatant (cytosolic extract) was transferred to a fresh tube on ice. Protein concentrations were quantified using the Quick Start™ Bradford Protein Assay Kit (#500-0203, Bio-Rad Laboratories, Inc., Foster City, CA, USA). Literally 100 μg protein was diluted into 50 μL Cell Lysis Buffer, and 50 μL of 2× Reaction Buffer containing 10 mM dithiothreitol (DTT) was next added to each sample. A final concentration of 200 μM of CASP3 substrate, Asp-Glu-Val-Asp-*p*-nitroanilide, was applied and further incubated at 37 °C for 2 h in the dark. Samples were read at 405 nm in a microtiter plate reader (Thermo Labsystems Multiskan Ascent 354, Lab Recyclers Inc., Gaithersburg, MD, USA). All experiments were triplicated and results are expressed as mean of the relative CASP3 activity ± SEM, after normalization to the control.

Immunoblotting analysis. Cell lysates were prepared with Radio-ImmunoPrecipitation Assay Buffer (#20-188, Millipore Corporation, Temecula, CA, USA). Lysates containing equal amounts of protein were separated by 12 or 15% SDS-polyacrylamide gel electrophoresis and electroblotted onto the polyvinylidene fluoride membrane (Immobilon™-P Transfer Membrane; Millipore). The filters were individually probed with the primary anti-human antibodies, including anti-poly (ADP-ribose) polymerase 1 (anti-PARP1; 1:1000, #9542, Cell Signaling Technology, Irvine, CA, USA), anti-phospho(Ser139)-H2A histone family, member X [anti-pH2AFX(Ser139); 1:500, #07-164, Upstate Biotechnology Inc. Lake Placid, NY, USA], anti-BAX (1:400, #sc-493, Santa Cruz Biotechnology Inc., Santa Cruz, CA, USA), anti-BBC3 (1:1000, #ab9543, Abcam, Cambridge, UK), anti-BH3 interacting domain death agonist (anti-BID; 1:200, #sc-11423, Santa Cruz), anti-CASP8 (1:1000, #9746, Cell Signaling), anti-CASP9 (1:1500, #9508, Cell Signaling), anti-CASP3 (1:500, #9602, Cell Signaling), anti-TP53 (1:200, #sc-162, Santa Cruz), anti-phospho(Ser15)-TP53 [anti-pTP53(Ser15); 1:1000, #9286, Cell Signaling), anti-TP63 (1:500, #sc-8344, Santa Cruz), anti-TP73 (1:1000, #1636-1, Epitomics Inc., Burlingame, CA, USA), anti-BCL2 (1:100, #sc-509, Santa Cruz), anti-PMAIP1 (1:250, #IMG-349A, Imgenex Corporation, San Diego, CA, USA), anti-cytochrome *c* oxidase subunit IV isoform 1 (anti-COX4I1; 1:2000, #A21347, Molecular Probes Inc., Eugene, OR, USA), anti-CYCS (1:500, #556433, BD BioSciences, San Jose, CA, USA) and anti-β-actin (1:3000, #MAB1501, Chemicon, Temecula, CA, USA; loading control). Protein bands were detected by Western Lightning™ Chemiluminescent Reagent Plus Kit (Perkin-Elmer Life Sciences, Boston, MA, USA) with horseradish-peroxidase-labeled secondary antibody [anti-mouse (#11503062) or anti-rabbit (#11503045), Jackson ImmunoResearch, West Grove, PA, USA] and visualized on a VersaDoc Image System (Bio-Rad). Conditions were optimized for each primary and secondary antibody. The intensity of bands in immunoblotting assays was quantified by densitometry in each lane and normalized to β-actin.

Measurement of the mitochondrial membrane potential. Cells were treated with 0 (DMSO, control), 10 (SK-Hep1) or 25 (Hep-3B) μM GTN for 4, 12, 24, 36 and 48 h, and incubated with 40 nM 3,3′-dihexyloxacarbocyanine iodide [$DiOC_6(3)$] for 30 min at 37 °C, followed by washing with ice-cold phosphate buffered saline (PBS). Cell pellets were thereafter collected and suspended in 500 μL of Ca^{2+}/Mg^{2+}-free PBS; fluorescent intensities of cells were analyzed by flow cytometry, as respective wavelengths for excitation and emission of 484 and 500 nm.

Detection on the accumulation of intracellular ROS. Intracellular ROS generation was measured by flow cytometry, followed by staining with 2,7-dichlorodihydrofluorescein diacetate (H_2DCFDA), which is specific for H_2O_2 (Narayanan et al., 1997). In brief, 5×10^4 cells were seeded in 12-well plates, allowed to attach overnight, and exposed to 0 (DMSO, control), 10 (SK-Hep1) or 25 (Hep-3B) μM GTN for different time periods (2 to 36 h). Cells were next stained with 5 μM H_2DCFDA for 30 min at 37 °C in the dark, and obtained for the fluorescence analyzed using an IPICS® XL-MCL™ flow cytometer (Beckman Coulter).

Alkaline comet assay and N-acetylcysteine treatments. Alkaline comet assay was carried out as previously described (Tice et al., 2000). Briefly, cells were seeded in six-well plates and treated with 0 (DMSO, control), 10 (SK-Hep1) or 25 (Hep-3B) μM GTN for 4 h. In order to determine the order between ROS formation and DNA damage in cells after GTN treatment, one ROS inhibitor, N-acetylcysteine (NAC; 2 mM) was pretreated for 1 h and then treated with GTN for another 4 h. Following incubation, detached cells in the medium were collected as well as the trypsinized cells (700 × *g*, 5 min at 4 °C). The supernatant was removed, the pellet was washed with Ca^{2+}/Mg^{2+}-free PBS and recentrifuged. The pellets were mixed thoroughly with 200 μL of 1.5% NuSieve® GTC® low melting point agarose (LMPA; FMC BioProducts, Rockland, ME, USA) and the mixture was pipetted onto hardened 1.5% Vegonia normal melting point agarose (Bertec Enterprise, Taipei, Taiwan) as the first layer of gel on the slide. A coverslip was placed to spread the mixture and the slide was left on ice to allow the LMPA to solidify. After removal

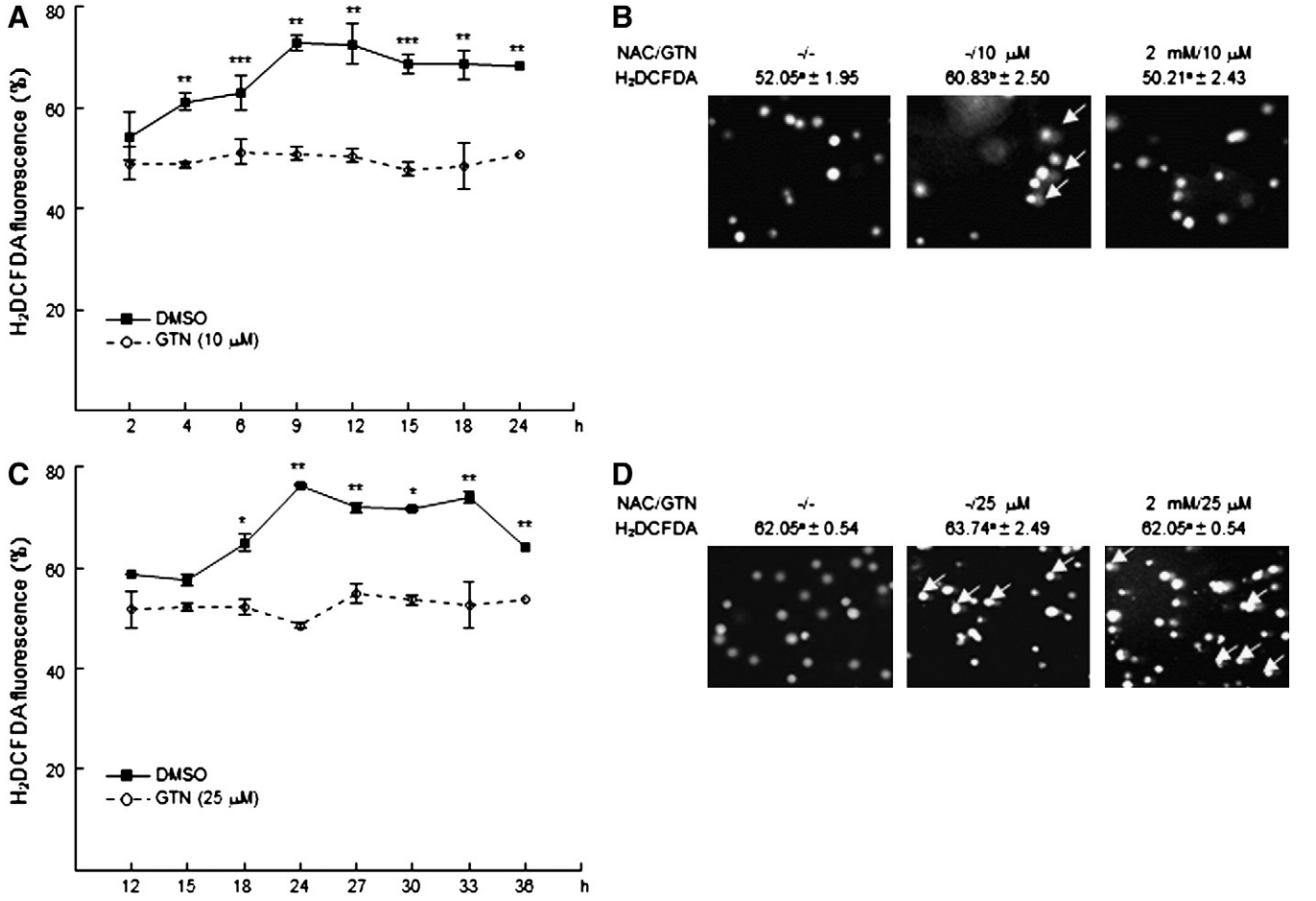

Fig. 4. GTN induced intracellular ROS formation and DNA damage in TP53-positive SK-Hep1 and TP53-negative Hep-3B cells. Cells were treated with 0 (DMSO, control), 10 (SK-Hep1) or 25 (Hep-3B) μM GTN for indicated time periods. GTN treatment for 4 h and 18 h induced ROS formation in (A) SK-Hep1, and (C) Hep-3B cells, respectively. (B, D) After treatment with GTN for 4 h, DNA damage in both cell lines was triggered, however, ROS was only induced in SK-Hep1 cells. Pretreatment with NAC inhibited GTN-induced ROS formation as well as DNA damage in SK-Hep1 cells, nevertheless, did not inhibit GTN-induced DNA damage in Hep-3B. All experiments were triplicated and results are expressed as mean ± SEM. Statistical significance between the treated group and its corresponding control: $^{*}P<0.05$; $^{**}P<0.01$ and $^{***}P<0.001$.

of the coverslip, embedded cells were lysed in the buffer containing 2.5 M NaCl, 100 mM Na_2EDTA, 10 mM Tris and 1% Triton X-100 (pH 10) at 4 °C overnight. Slides were soaked in electrophoresis buffer (300 mM NaOH, 1 mM EDTA, pH 13) for 20 min to unwind DNA before electrophoresis at 300 mA, 25 V for 20 min. Subsequently, slides were rinsed with neutralizing buffer (0.4 M Tris–HCl, pH 7.5) for 5 min and stained with 50 μL 4′,6-diamidino-2-phenylindole (DAPI; 1 μg/mL) solution. Slides were left overnight at 4 °C before analyzing under the DM IRB fluorescent microscope equipped with a 590-nm filter (Leica Microsystems, Wetzlar, Germany) and representative images were photographed.

Immunocytochemistry. Cells were grown on coverslips, which were precoated with 1% gelatin for 30 min before seeding. After treatment with DMSO (control) or GTN for 24 h, cells were washed with PBS, fixed in 3.7% formaldehyde (in PBS) for 5 min, and 0.3% triton X-100 for 15 min at room temperature. With each step forward, cells were washed with PBS three times, next blocked with PBS containing 1% bovine serum albumin and kept overnight at 4 °C. The primary anti-pH2AFX (Ser139) antibody (1:100) was applied for 1 h at room temperature. Unbounded antibodies were washed with PBS, and FITC-labeled secondary antibody (1:200; #115-095-003, Jackson Laboratory, Bar Harbor, ME, USA) was applied for another 1 h at room temperature, rinsed with PBS and stained with DAPI (1 μg/mL) for 5 min. Following a series of washes, cells were mounted, viewed with appropriate filters and photographed by an Axioskop 2 plus microscope (Carl Zeiss, Goettingen, Germany).

Plasmid-based small-hairpin RNA interference targeting PMAIP1 and TP53 genes. Clones of small-hairpin RNA (shRNA) interference plasmids, purchased from the National RNAi Core Facility (Institute of Molecular Biology, Academia Sinica, Taipei, Taiwan) have been inserted into the pLK0.1 vector downstream of the U6 promoter. Five shPMAIP1 and another five shTP53 clones targeting *PMAIP1* and *TP53* genes, respectively, were preliminarily screened. For each target transcript, the mRNA level could be effectively downregulated by only two and one clones, which were designed as the shPMAIP1 #1 and PMAIP1 #4; and shTP53 #1 in further experiments. The sense strand sequences of RNA duplexes were as follows: shPMAIP1 #1 (TRCN0000150555: 5′-GCATTGTTGTTGTTGCTGTTT-3′), shPMAIP #4 (TRCN0000155570: 5′-CTTCCGGCAGAAACTTCTGAA-3′), shTP53 #1 (TRCN0000010814: 5′-GAGGGATGTTTGGGAGATGTA-3′), and the negative control, shLuc (TRCN0000072243: 5′-CTTCGAAATGTCC-GTTCGGTT-3′). Cells at a density of 10^5 were seeded in six-well plates and transfected with 2 μg of shPMAIP1 #1, shPMAIP1 #4 or shTP53 #1 plasmid in 6 μL TransFast™ Transfection Reagent (Promega Corporation, Madison, MI, USA). After transfection, cells were incubated at room temperature for 20 min and further maintained in a 37 °C, 5% CO_2 incubator with culture medium to 4 d for the shPMAIP1 and 9 d for the shTP53 plasmid, correspondingly, before

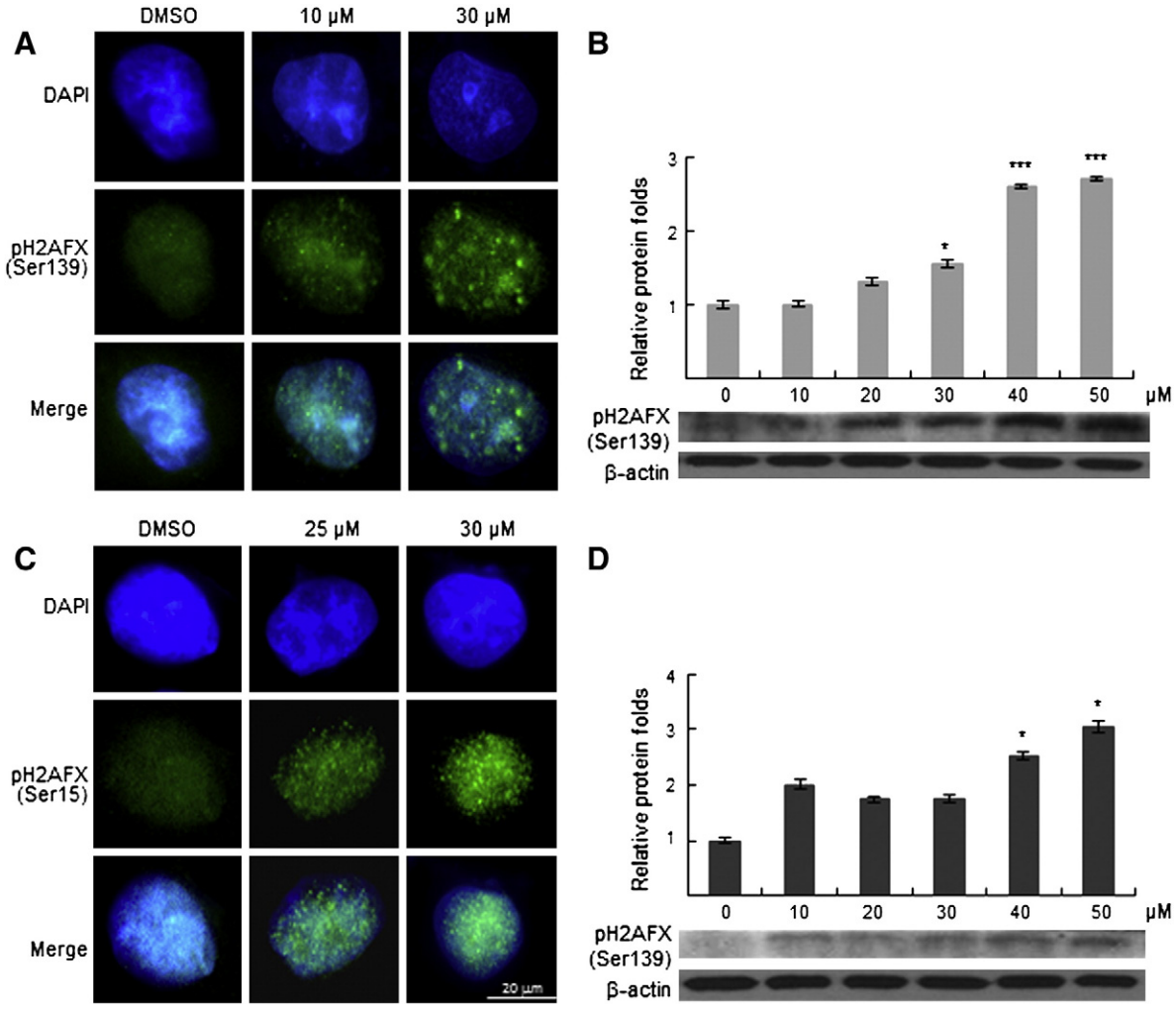

Fig. 5. GTN induced double-strand breaks in TP53-positive SK-Hep1 and TP53-negative Hep-3B cells. (A, C) GTN induced the formation of pH2AFX(Ser139) foci, and (B, D) pH2AFX (Ser139) protein levels in a dose-dependent manner in both SK-Hep1 (A, B) and Hep-3B (C, D) cell lines. All experiments were triplicated and immunoblotting quantifications are expressed as mean ± SEM. For immunoblotting analysis, the β-actin was also examined for the loading control. One representative immunocytochemical image (A, C) and immunoblotting image is shown (B, D).

analyses. The alterations in expression levels of *PMAIP1* and *TP53* transcripts and protein abundances of PMAIP1, TP53, pTP53(Ser15) and PARP1, as well as the percentage of apoptotic cells were analyzed for shPMAIP1- or shTP53-transfected versus shLuc-transfected cells (control) in the absence or presence of GTN, by quantitative reverse transcription-polymerase chain reaction (RT-PCR), immunoblotting and flow cytometric assays.

Preparation of cDNA and quantitative RT-PCR. Total RNA from cells was isolated using Trizol reagent (Gibco Invitrogen). The cDNA was synthesized with oligo(dT)$_{15}$ primers, Moloney Murine Leukemia Virus reverse transcriptase (Promega), and quantified at OD_{260}/OD_{280}. The iCycler thermal cycler (Bio-Rad) was used to quantify the relative [to glyceraldehyde-3-phosphate dehydrogenase (*GAPDH*)] expression levels of *PMAIP1* (5′-CATGAGGGGACTCCTTCAAA-3′, 5′-TTCCATCTTCCGTTTCCAAG-3′; 4 μM; 129 bp; NM_021127) and *TP53* (5′-CGTACTCCCCTGCCCTCAAC-3′, 5′-GTGCTGTGACTGCTTGTAGATGG-3′; 1 μM; 131 bp; NM_000546), and the internal control *GAPDH* (5′-ACCCAGAAGACTGTGGATGG-3′, 5′-TTCTAGACGGCAGGTCAGGT-3′; 4 μM; 201 bp; NM_002046) transcripts in the cells with SYBR Green I labeling (Absolute QPCR SYBR Green Mix; ABgene, Epsom, UK). The efficiency of each primer set was validated to be equivalent as in our previous study (Shiue et al., 2006) (see also Supplementary Fig. S2 in the online version of this article). Equal amount from an aliquot of each sample was pooled to be a common reference cDNA for further calculation of relative expression levels of each transcript. Quantitative RT-PCRs were performed in a total volume of 15 μL [7.5 μL SYBR Green Mix and 0.75 μL (concentration was optimized by specific transcript) of forward and reverse primers, and 6 μL (12.5 ng/μL) cDNA]. The reaction was performed at 95 °C for 10 s, annealing at 58 °C (*PMAIP1* vs. *GAPDH*) or 60 °C (*TP53* vs. *GAPDH*) for 5 s, and elongation at 72 °C for 12 s in 96-well plates. The starting copy number of unknown cDNA samples was determined relative to the copy number of the calibrator sample (common reference cDNA) using the following formula: $\Delta\Delta Ct = \Delta Ct[(\text{target, unknown sample}) - (\textit{GAPDH}, \text{unknown sample})] - \Delta Ct[(\text{target, common reference cDNA}) - (\textit{GAPDH}, \text{common reference cDNA})]$. The relative mRNA expression fold was calculated by the expression $2^{-\Delta\Delta Ct}$. All reactions were triplicated and results are expressed as mean ± SEM.

Mitochondria/cytosol fractionation. Mitochondria and cytosol were isolated by using Mitochondria/Cytosol Fractionation Kit (#K256-25; BioVision) according to the manufacture's protocols. Briefly, 10^6 cells were centrifuged and washed with PBS (700×*g*, 5 min) at 4 °C, the supernatants were removed. Cells were resuspended with 200 μL 1× Cytosol Extraction Buffer Mix containing DTT and protease inhibitor cocktail, and incubated for 30 min on ice. Cells were next

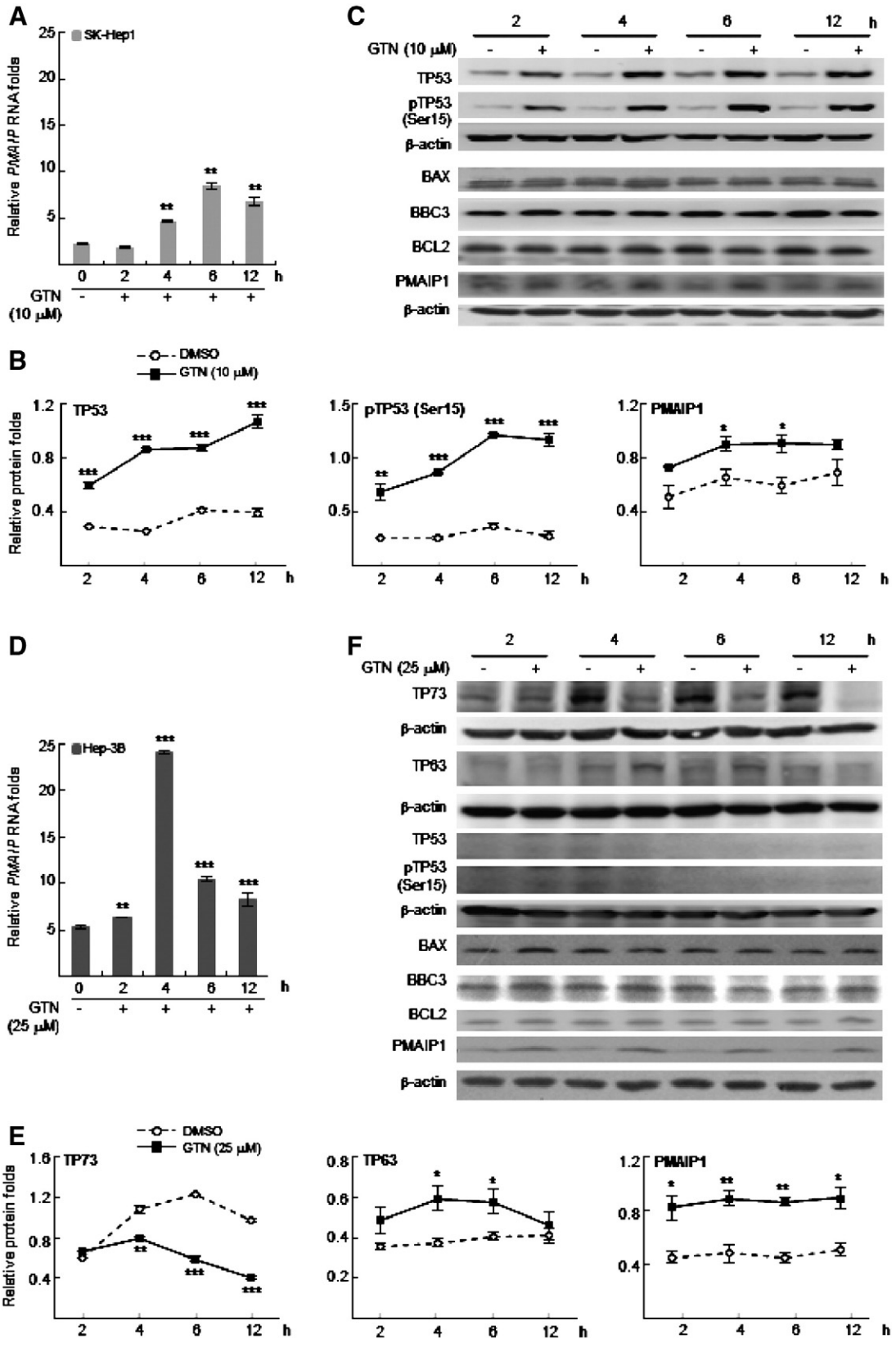

Fig. 6. GTN induced apoptosis via *PMAIP1* upregulation in TP53-positive SK-Hep1 and TP53-negative Hep-3B cells. Treatments with GTN for 4 to 12 h in SK-Hep1 cells (A), and for 2 to 12 h in Hep-3B cells (D), induced *PMAIP1* mRNA levels. (B, C) In SK-Hep1 cells, treatments with GTN for 2 to 12 h induced TP53 and pTP53(Ser15) protein levels; for 4 to 6 h induced *PMAIP1* protein levels. Treatments with GTN for 4 to 12 h suppressed TP73; for 4 to 6 h induced TP63 protein levels; for 2 to 12 h induced *PMAIP1* protein levels in Hep-3B cells (E). Transfection of shRNA plasmids (shPMAIP1 #1 and #4) targeting the *PMAIP1* gene suppressed *PMAIP1* mRNA levels (G, H), *PMAIP1* protein abundance (I, J), as well as GTN-induced (24 h) percentages of apoptotic cells (K, L) in both cell lines. All experiments were triplicated and results are expressed as mean SEM. For immunoblotting analysis, the -actin was also examined as the loading control and one representative image is shown (C, F, I and J). Statistical significance: $^{*}P<0.05$; $^{**}P<0.01$; $^{***}P<0.001$; ^{ae}within an experiment, values without a common superscript differed ($P<0.05$).

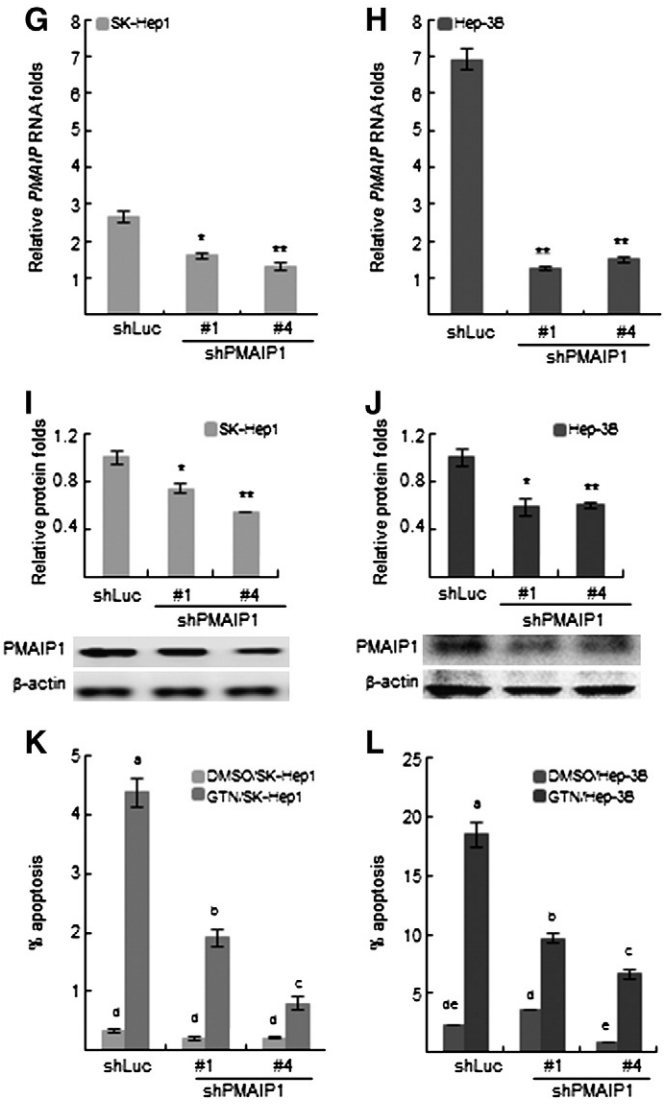

Fig. 6 (*continued*).

homogenized (60 strokes) in an ice-cold Dounce Tissue Grinder (#1998-1, BioVision), transferred to a 1.5-mL microcentrifuge tube and centrifuged (10,000×*g*, 30 min) at 4 °C. The supernatant was collected as cytosolic fraction and stored at −80 °C before analysis. The mitochondrial faction in the pellet was vortexed with 200 μL of the Mitochondrial Extraction Buffer Mix containing DTT and protease inhibitor cocktail and stored at −80 °C before analysis.

Statistics. The Student's *t*-test or Fisher's least significant difference was used to examine the statistical significance of alternations on the apoptotic cell percentage, relative CASP3 activity, mitochondrial transmembrane potential, ROS formation, the relative mRNA and protein levels, between or among different groups. All calculations were performed by SPSS 14.0 software (SPSS Inc., Chicago, IL, USA).

Results

GTN induced apoptosis in HCC-derived cells

Half maximal inhibitory concentrations (IC_{50}) of GTN in TP53-posivive SK-Hep1 and TP53-negative Hep-3B cells were determined as 10 and 25 μM (48 h) by the 3-(4,5-Dimethylthiazol-2-yl)-2,5-diphenyltetrazolium bromide assay (see Supplementary Fig. S1B, S1C in the online version of this article). In order to analyze GTN-induced apoptosis as early as possible, these concentrations were used for subsequent experiments, except for dose–response experiments. After treatment of 0 (DMSO, control), 10, 20 or 40 μM GTN for 24 h, dose-dependent early apoptosis was induced in SK-Hep1 ($P<0.01$; Fig. 1A) and Hep-3B ($P<0.05$; Fig. 1B) cells. Late apoptosis was also induced by GTN in a dose-dependent manner in both cell lines (10 or 20 to 40 μM, $P<0.05$; Fig. 1).

GTN induced CASP-mediated apoptosis in HCC-derived cells

In SK-Hep1, GTN treatments for 24 h induced the cleavages of CASP8, CASP9, CASP3 and PARP1 proteins in a dose-dependent manner (Fig. 2A). However, only cleaved-CASP8 and -CASP3 were induced by GTN in Hep-3B cells (Fig. 2B). GTN treatment for 24 h further increased the percentage of apoptotic cells ($P<0.01$ and $P<0.001$; Fig. 2C, D) and CASP3 activities ($P<0.01$; $P<0.001$; Fig. 2E, F) in both cell lines, compared to those of controls. Pretreatment with a pan CASP inhibitor, z-VAD-FMK (50 μM), in SK-Hep1 and Hep-3B cells for 1 h, repressed endogenous ($P<0.05$; $P<0.001$) and GTN-induced (10 and 25 μM GTN for SK-Hep1 and Hep-3B cells, respectively, for 24 h) percentages of

apoptotic cells ($P<0.001$; $P<0.001$; Fig. 2C, D); endogenous ($P<0.05$; $P<0.05$) and GTN-induced CASP3 activities ($P<0.01$; $P<0.001$; Fig. 2E, F). In addition, z-VAD-FMK noticeably reduced GTN-induced PARP1 cleavages in both cell lines ($P<0.01$; Fig. 2G, H).

GTN impaired the integrity of mitochondrial membranes in HCC-derived cells

Time-course experiment (GTN treatments) and flow cytometric assay were performed to determine the $DiOC_6(3)$ fluorescence intensities in HCC-derived cell lines. Results reflected the collapse of mitochondrial membrane potentials and integrities as early as 12 h after GTN treatments in TP53-positive SK-Hep1 ($P<0.001$; Fig. 3A) and TP53-negative Hep-3B ($P<0.01$; Fig. 3B) cells. After treatment with GTN for 48 h, the percentages of cells with impaired mitochondrial membrane integrity attained 13.25% ($P<0.001$; Fig. 3A) and 12.20% ($P<0.001$; Fig. 3B) in SK-Hep1 and Hep-3B cells, respectively.

GTN induced intracellular ROS formation and DNA damage in HCC-derived cells

Treatment with GTN (IC_{50}) induced intracellular ROS formation after 4 and 18 h in TP53-positive SK-Hep1 ($P<0.01$) and TP53-negative Hep-3B ($P<0.05$) cells (Fig. 4A, C). 24 h induced DNA damage response in both cell lines (see Supplementary Fig. S3 in the online version of this article). In addition, NAC suppressed GTN-

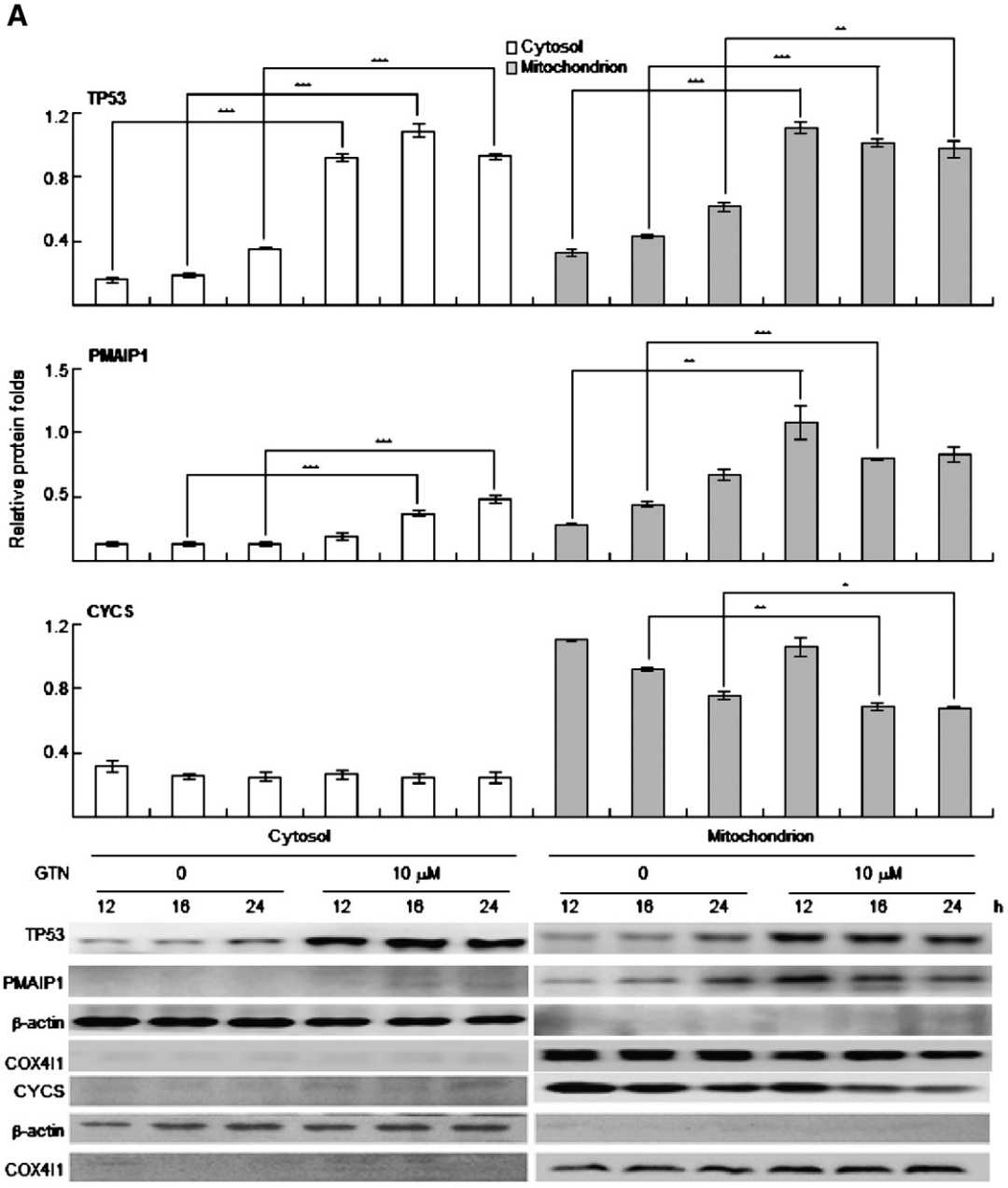

Fig. 7. GTN induced mitochondrial CYCS release in TP53-positive SK-Hep1 and TP53-negative Hep-3B cells via upregulation of mitochondrial TP53 and/or PMAIP1 proteins. (A) In SK-Hep1 cells, mitochondrial TP53 and PMAIP1 protein levels were upregulated after GTN treatments for 12 to 24 h and 12 to 16 h, respectively. Mitochondrial CYCS decreased after treatment with GTN for 16 to 24 h. (B) In Hep-3B cells, mitochondrial PMAIP1 protein levels were increased after GTN treatments for 12 to 24 h. Mitochondrial CYCS decreased after treatment with GTN for 12 to 24 h. All experiments were triplicated and one representative immunoblotting image is shown. Immunoblotting quantifications are expressed as mean ± SEM. The β-actin (cytosol-specific) and COX4I1 (mitochondrion-specific) were detected as controls.

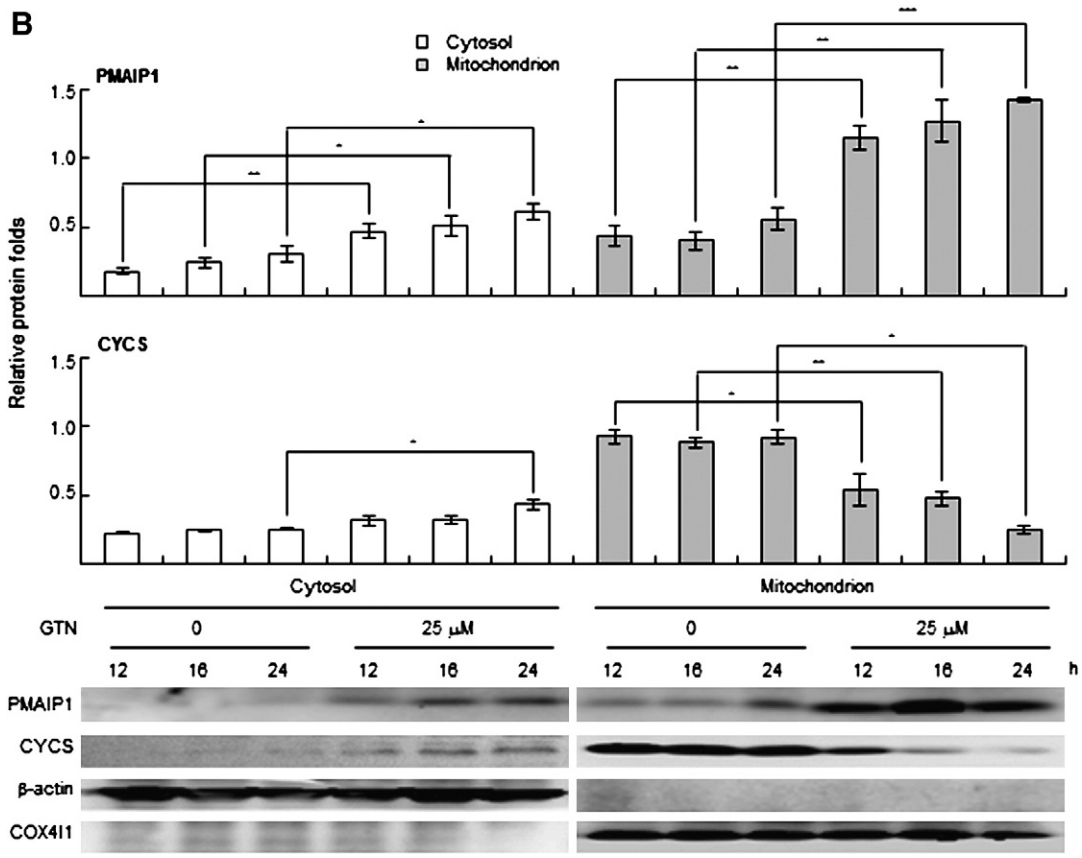

Fig. 7 (*continued*).

induced (4 h) ROS formation, as well as DNA damage in SK-Hep1 ($P<0.05$; Fig. 4B). However, it was not able to suppress GTN-induced (4 h) DNA damage in Hep-3B cells (Fig. 4D). In both cell lines, immunocytochemistry and immunoblotting analysis further demonstrated that GTN treatments for 24 h induced the formation of pH2AFX(Ser139) foci (Fig. 5A, C) and pH2AFX(Ser139) protein abundance (Fig. 5B, D) in a dose-dependent manner.

GTN induced apoptosis via transactivation of the PMAIP1 gene in HCC-derived cells

In SK-Hep1 cells, semi-quantitative RT-PCR identified that GTN treatment induced *PMAIP1* transcription among a series of BCL-family genes in a dose-dependent manner (see Supplementary Fig. S4 in the online version of this article). Quantitative RT-PCR further demonstrated that after GTN treatment for 4 h, the *PMAIP1* mRNA level reached the climax in Hep-3B cells ($P<0.001$; Fig. 6D), earlier than that of SK-Hep1 cells (6 h, $P<0.01$; Fig. 6A). Expression levels of several proapoptotic and antiapoptotic proteins were afterward examined by the immunoblotting analysis to determine whether GTN-induced apoptosis was mitochondria-mediated. In SK-Hep1 cells, protein levels of TP53 ($P<0.001$), pTP53(Ser15) ($P<0.01$) and PMAIP1 ($P<0.05$) were considerably upregulated after GTN treatments for 2, 2 and 4 h, respectively. In the meanwhile, most upregulated TP53 proteins was the pTP53(Ser15) (Fig. 6B, C). In TP53-negative Hep-3B cells, PMAIP1 was induced after GTN treatment for 2 to 12 h ($P<0.05$). On the other hand, TP73 was suppressed in a dose-dependent manner ($P<0.01$) but TP63 protein abundance was slightly induced after GTN treatments for 4 to 6 h ($P<0.05$; Fig. 6E, F). Neither E2F transcription factor 1 (E2F1) nor v-myc myelocytomatosis viral oncogene homolog (avian) (MYC) protein was stimulated by GTN in the dose–response experiment in both cell lines (see Supplementary Fig. S5 in the online version of this article).

Two shPMAIP1 clones (shPMAIP1 #1 and #4) able to effectively knockdown the *PMAIP1* gene were further used to suppress the endogenous *PMAIP1* mRNA levels in both cell lines. After *PMAIP1* knockdown, quantitative RT-PCR and immunoblotting analysis demonstrated that the *PMAIP1* mRNA ($P<0.05$; Fig. 6G, H) and protein (Fig. 6I, J) levels were downregulated in TP53-positive SK-Hep1 and TP53-negative Hep-3B cells. Additionally, knockdown of the *PMAIP1* gene suppressed GTN-induced percentages of apoptotic cells, compared to those of the shLuc-transfected control groups in both cell lines ($P<0.05$; Fig. 6K, L).

GTN upregulated mitochondrial TP53 and/or PMAIP1 protein level, and induced the release of mitochondrial CYCS in HCC-derived cells

Mitochondria/cytosol fractionation and immunoblotting analysis were performed to examine the effects of GTN treatment on the subcellular localization of CYCS, TP53 and/or PMAIP1 proteins in TP53-positive SK-Hep1 and TP53-negative Hep-3B cells. In a time-dependent manner, GTN notably upregulated mitochondrial TP53 and PMAIP1 protein levels in SK-Hep1 cells (Fig. 7A), and PMAIP1 protein abundance in Hep-3B cells (Fig. 7B). In both cell lines, GTN treatment also induced mitochondrial CYCS release into the cytosol in a time-dependent manner (Fig. 7A, B). However, GTN could not induce the mitochondrial TP63 levels in TP53-negative Hep-3B cells (see Supplementary Fig. S6 in the online version of this article).

Knockdown of TP53 gene suppressed GTN-induced pTP53, pTP53(Ser15), PMAIP, cleaved PARP1 protein levels and the percentage of apoptotic cells in SK-Hep1 cells

As shown in Fig. 8A, *TP53* mRNA levels were upregulated after the GTN treatment for 2 to 12 h ($P<0.05$); reached the apex after treatment for 4 h ($P<0.01$). On the other hand, treatment with a specific inhibitor (PFT-α) of TP53 transcriptional activity (Murphy

et al., 2004) in SK-Hep1 cells, markedly downregulated endogenous pTP53(Ser15) ($P<0.05$) and PMAIP1 ($P<0.05$), as well as GTN-induced TP53 ($P<0.01$), pTP53(Ser15) ($P<0.001$), PMAIP1 ($P<0.001$), and cleaved-PARP1 ($P<0.001$) protein levels (Fig. 8B, C). In the absence of GTN, PFT-α treatment increased the endogenous percentage of apoptotic cells ($P<0.05$); slightly but not significantly enhanced GTN-induced percentage of apoptotic cells ($P=0.07$; Fig. 8D).

Transfection of the shTP53 plasmid into SK-Hep1 cells to knockdown the *TP53* gene downregulated endogenous *TP53* ($P<0.01$) as well as *PMAIP1* ($P<0.01$) mRNA levels, compared to the corresponding shLuc-transfected control group (Fig. 8E). Transfection of the shTP53 plasmid in the absence of GTN, protein levels of TP53 ($P<0.05$), pTP53(Ser15) ($P<0.05$) and PMAIP1 ($P<0.05$); in the presence of GTN, protein levels of TP53 ($P<0.01$), pTP53(Ser15) ($P<0.05$), PMAIP1 ($P<0.05$) and cleaved-PARP1 ($P<0.01$) were repressed, compared to the corresponding shLuc-transfected control group (Fig. 8E, F). Without GTN treatment, the endogenous percentage of apoptotic cells was inhibited by knockdown of the *TP53* gene ($P<0.05$); *TP53* knockdown further reduced the GTN-induced percentage of apoptotic cells ($P<0.05$) (Fig. 8H). Molecular mechanisms underlying GTN-induced apoptosis in TP53-positive SK-Hep1 and TP53-negative Hep-3B cells is summarized in Fig. 9.

Discussion

We identified the involvement of PMAIP1 in GTN-induced apoptosis via TP53-dependent and -independent pathways in HCC-derived cells. GTN is a natural proapoptotic compound, that was found to induce ROS formation; DNA double-strand breaks; *TP53* and/or *PMAIP1* transactivation, translation, and translocation to mitochondria; alterations in the mitochondrial membrane potential; release of mitochondrial CYCS; cleavage of CASP8, CASP9, CASP3, and PARP1; and consequential apoptosis in TP53-positive SK-Hep1 and TP53-negative Hep-3B cells. This is followed by cleavage of PARP1 in vivo due to CYCS release, formation of apoptosomes, and the activation of CASP9 and CASP3. It has been suggested that PARP1 cleavage as a result of CYCS release is an apoptosis-specific event and aims at stopping the activity of high energy consuming PARP1, thereby preventing energy depletion and uncontrolled cell death caused by

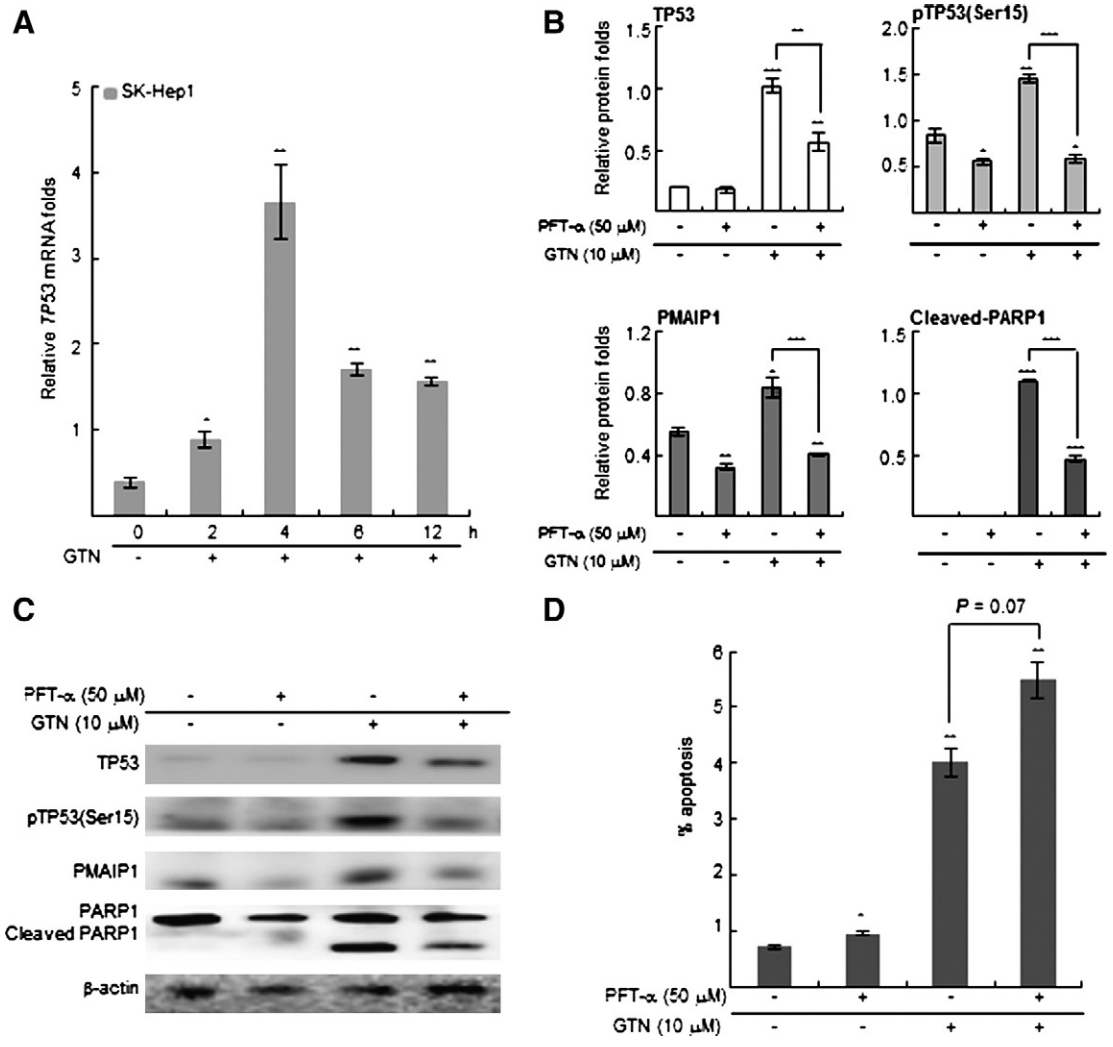

Fig. 8. Knockdown of the *TP53* gene suppressed GTN-induced *TP53* and *PMAIP1* mRNA levels; TP53, pTP53(Ser15), PMAIP1 and cleaved-PARP1 protein abundances and the percentage of apoptotic cells in TP53-positive SK-Hep1 cells. (A) GTN treatment for 2 to 12 h induced *TP53* mRNA levels. (B–D) Pretreatment with a TP53 inhibitor, PFT-α, for 1 h, suppressed GTN-induced TP53, pTP53(Ser15), PMAIP1 and cleaved-PARP1 protein levels; slightly but not significantly enhanced the percentage of apoptotic cells. Knockdown of *TP53* gene suppressed *TP53* and *PMAIP1* mRNA expression folds, compared to their corresponding shLuc-transfected control groups (E). (F–H) Cells were treated with 0 (DMSO, control) or 10 μM GTN for 24 h, in conjunction with transfection of shLuc (control) or shTP53 plasmid. Knockdown of *TP53* in the absence or presence of GTN repressed endogenous, GTN-induced TP53, pTP53(Ser15) and PMAIP1 protein levels; additionally diminished GTN-induced cleavage of the PARP1 protein. Knockdown of *TP53* gene also reduced endogenous and GTN-induced percentage of apoptotic cells. All experiments were triplicated and results are expressed as mean ± SEM. One representative immunoblotting image is shown (C, G) and β-actin served as the loading control. Statistical significance: $^{*}P<0.05$; $^{**}P<0.01$ and $^{***}P<0.001$.

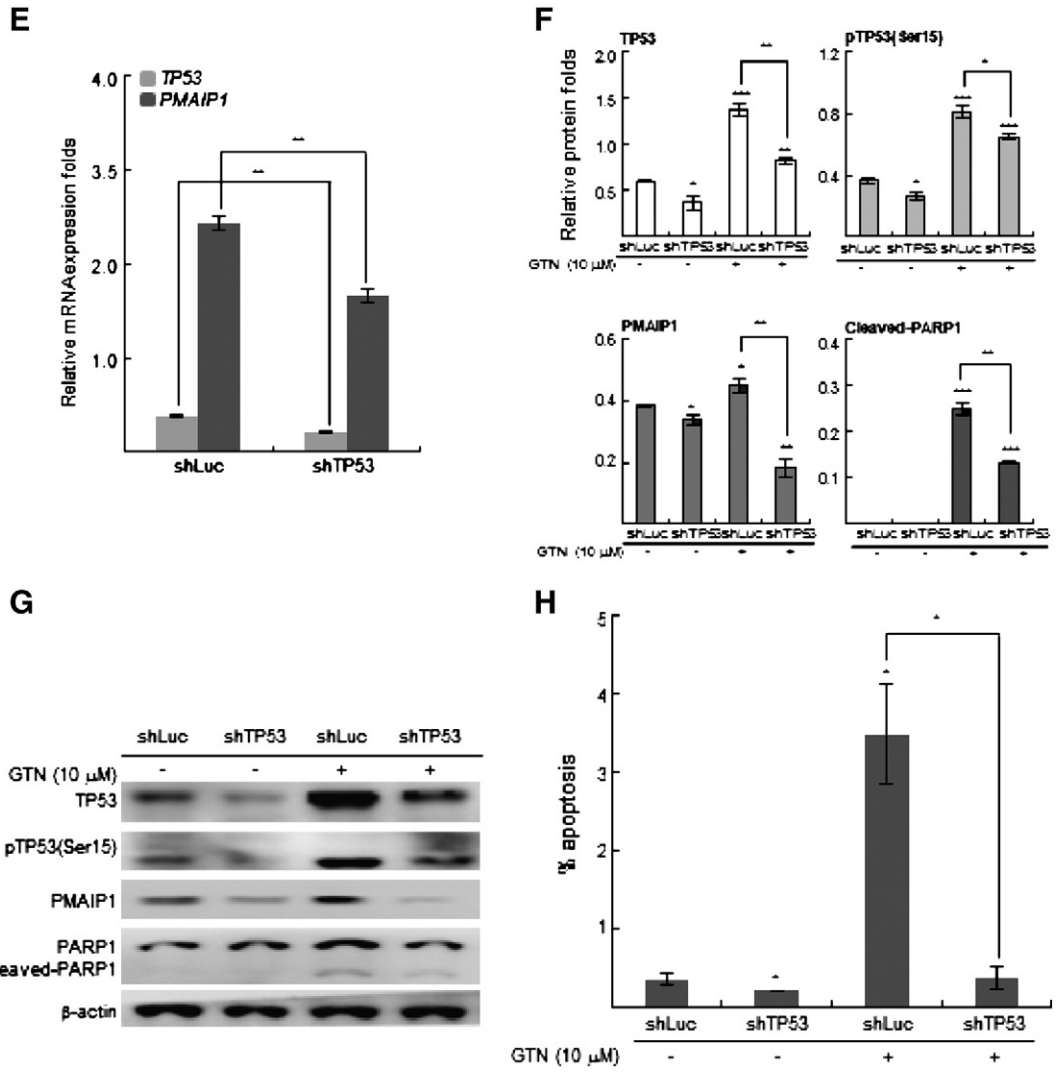

Fig. 8 (*continued*).

necrosis (D'Amours et al., 2001). We confirmed that GTN induces mitochondrial apoptosis in HCC-derived cells via activation of the *TP53* and/or *PMAIP1* genes.

Our results clearly indicate that GTN induced transactivation and translation of the TP53 gene and subsequent transactivation of the *PMAIP1* gene in TP53-positive SK-Hep1 cells. This is because (1) the TP53 protein level increased notably 2 h after the GTN treatment as compared to the PMAIP1 level, which increased 4 h after the GTN treatment; (2) the *TP53* mRNA level reached the maximum (3.65-fold) 4 h after GTN treatment, as compared to the mRNA level of *PMAIP1*, which reached the maximum (5.56-fold) 6 h after GTN treatment; (3) knockdown of the *TP53* gene significantly suppressed both *TP53* and *PMAIP1* mRNA levels when compared to their corresponding controls; and (4) regardless of the absence or presence of GTN, knockdown of *TP53* notably suppressed TP53 and PMAIP1 protein expression when compared to the corresponding shLuc-transfected control groups.

On the other hand, in TP53-deficient Hep-3B cells, GTN significantly induced an increase in *PMAIP1* mRNA and protein expression, as early as 2 h after the treatment. Because GTN increase in *PMAIP1* mRNA and protein levels prior to that of another TP53 protein member, TP63 protein, the potential regulatory role of TP63 in *PMAIP1* was excluded. Either the *TP53* or *PMAIP1* gene has been reported as potential drug target in several tumor types, including HCCs (Ploner et al., 2008; Staib et al., 2003). Thus, activation of the *TP53* or *PMAIP1* gene product appears to be critical in the cellular responses to anticancer treatments. Although the *PMAIP1* gene can be also transactivated by other transcriptional factors such as E2F1 (Hershko and Ginsberg, 2004) or MYC (Nikiforov et al., 2007), these transcription factors were not found to be induced by GTN in both TP53-positive SK-Hep1 and TP53-negative cells in this study. Therefore, their potential regulatory roles were ruled out.

Results obtained from the alkaline comet assay as well as the pH2AFX(Ser139) protein level was upregulated soon after the GTN treatment, reconfirming that GTN induces DNA damage in HCC-derived cells. DNA double-stranded breaks present a serious challenge for eukaryotic cells. The inability to repair breaks leads to genomic instability, carcinogenesis and cell death. During the double-strand break response, mammalian chromatin undergoes reorganization demarcated by phosphorylation in Ser139 of H2AFX (Xiao et al., 2009). Therefore, formation of pH2AFX nuclear foci further indicated that GTN-induced DNA damage by creating double-strand breaks. The GTN-induced DNA damage subsequently stimulated the DNA repair proteins pTP53(Ser15) and/or proapoptotic protein PMAIP1 and resulted in the initiation of downstream mitochondria-mediated apoptosis, which was further supported by phosphatidylserine externalization. In addition to the fact that both R-roscovitine (a cyclin-dependent kinase inhibitor) and γ-irradiation are capable of

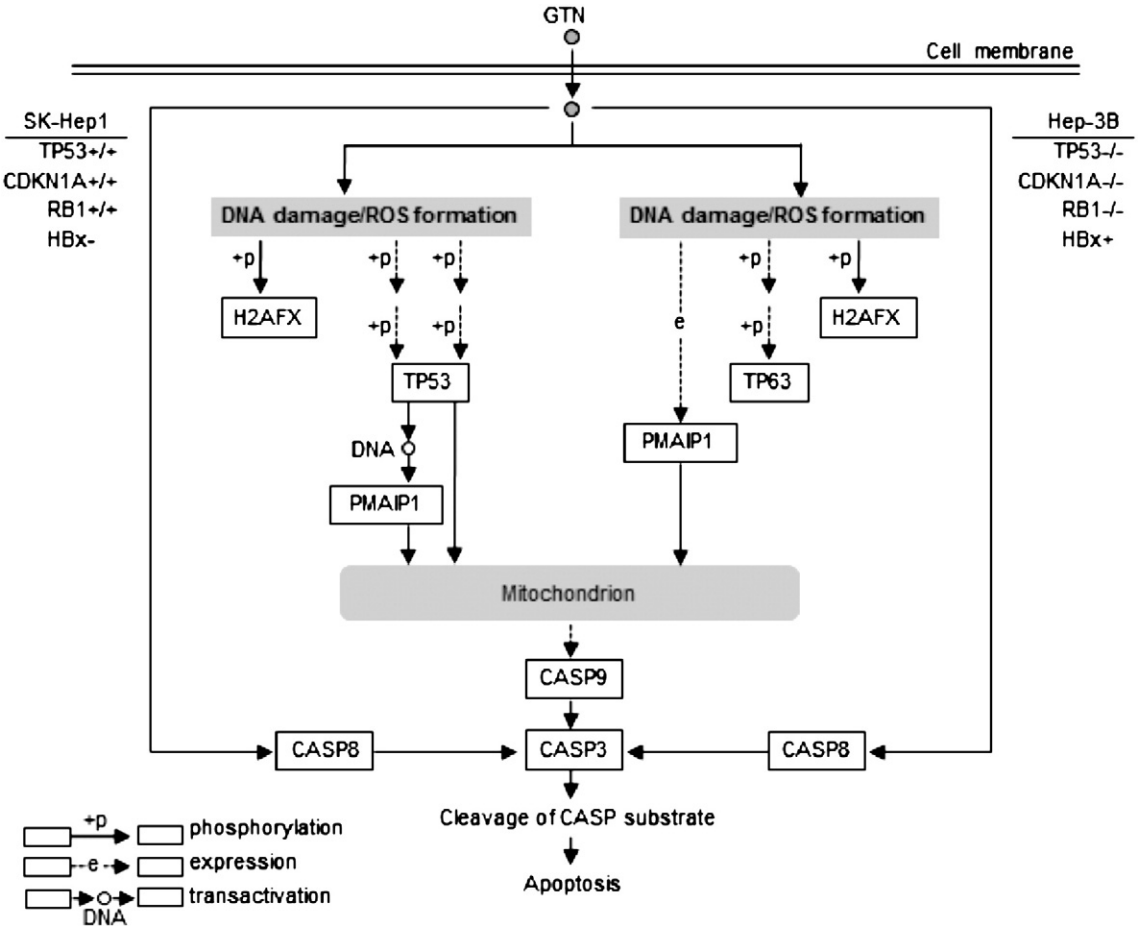

Fig. 9. Summary on the GTN-induced apoptotic pathways in TP53-positive SK-Hep1 and TP53-negative Hep-3B cells.

downregulating MCL1 (an antiapoptotic protein), histone deacetylase, and proteasome, as well as triggering de novo synthesis of PMAIP1 (Hallaert et al., 2007; Inoue et al., 2007), GTN-induced PMAIP1 expression might enhance the efficiency of the current treatment strategies against cancers.

Of the several BCL2 family proteins that were examined, mitochondrial TP53 and PMAIP1 protein levels and only PMAIP1 protein levels, were significantly upregulated in SK-Hep1 and Hep-3B cells, respectively, for 12 h after the GTN treatment, corresponding to the time point of significant reduction in the mitochondrial membrane integrity. Undeniably, PMAIP1 is probably a proapoptotic modifier rather than a tumor suppressor (Ploner et al., 2008). Overexpression of mouse *Pmaip1* in HeLa or other cancer cells results in significant apoptosis, which is associated with preferential localization of Pmaip1 to the mitochondria (Oda et al., 2000). Binding of PMAIP1 to the proapoptotic BAX or BAK1 protein has not been reported so far, indicating that PMAIP1 indirectly promotes BAX/BAK1-mediated mitochondrial dysfunction by inhibiting expression of the antiapoptotic members of the BCL2 family (Oda et al., 2000; Shibue et al., 2003). This implies that the *PMAIP1* gene in either TP53-positive SK-Hep1 or TP53-negative Hep-3B cells might also play a critical role in GTN-induced apoptosis.

Significant decrease in the percentage of GTN-induced apoptotic cells due to *PMAIP1* gene knockdown was consistent with the results obtained from other cellular and animal models. The role of PMAIP1 in the doxorubicin-induced neuroblastoma apoptosis was confirmed by *PMAIP1* knockdown experiments (Kurata et al., 2008). The *PMAIP1*$^{-/-}$ mice showed resistance to X-ray irradiation-induced gastrointestinal death, accompanied with impaired apoptosis of the epithelial cells of small intestinal crypts (Shibue et al., 2003). The inhibition of apoptosis was more profound in the *TP53*-knockdown SK-Hep1 cells than in the *PMAIP1*-knockdown SK-Hep1 cells, suggesting that in addition to *PMAIP1* transactivation, GTN-induced *TP53* expression might trigger apoptosis via other potential mechanisms.

In SK-Hep1 cells, PFT-α inhibited the GTN-induced increase in pTP53(Ser15), PMAIP1, and cleaved PARP1 protein levels, but there was no significant reduction in the percentage of GTN-induced apoptotic cells. Indeed, after GTN treatment, some amount of TP53 was still present in the cytosol and mitochondria, which might explain the previously described transcription-independent apoptotic function of cytosolic and mitochondrial TP53 (Speidel, 2010). A number of independent studies suggest that the tumor suppressor gene *TP53* plays a pivotal role in several DNA damage and growth control pathways (Kuerbitz et al., 1992; Livingstone et al., 1992). Generally, it is suggested that TP53 is activated following genotoxic stress; this triggers the DNA repair mechanism, leading to completion of the cell cycle. Alternatively, TP53 may also induce apoptosis leading to exit from the cell cycle. Several cellular models use DNA damaging agents such as γ-irradiation and cisplatin, which bring about the pTP53 (Ser15) level. Although this results in the reduction of DNA repair activity, there is a definite increase in the specific DNA binding activity and induction of apoptosis (Offer et al., 2002). There was a considerable increase in the levels of pTP53(Ser15) in SK-Hep1 cells, thereby strengthening the possibility that TP53 plays a transcription-independent role in GTN-induced apoptosis.

Consistent with our observations in HCC-derived cells, several studies using other tumor cells also suggested that GTN induces apoptosis but not necrosis (Chen et al., 2005; Inayat-Hussain et al., 1999; Inayat-Hussain et al., 2003; Inayat-Hussain et al., 2010). GTN is known to induce cytotoxicity and apoptosis in many cell lines at low

micromolar concentrations (Mereyala and Joe, 2001). The IC_{50} (48 h) of GTN identified in MCF-7, UACC-62, and HT-29 cells (Fatima et al., 2006) were similar to this study, reinforcing its potential in inhibition of cell growth in both TP53-positive or TP53-negative HCC-derived cells. The pan-caspase inhibitor represses GTN-induced CASP3 activity, abundance of cleaved PARP1 protein, and the percentage of apoptotic cells, supporting that the fact that GTN-induced apoptosis is CASP-mediated.

GTN induced ROS formation and subsequent DNA damage in TP53-positive SK-Hep1 cells, in the order opposite to that observed in TP53-negative Hep-3B cells. Because of its ability to induce chromatid- and chromosome-type aberrations in CHO cells, GTN is suggested to be a potential genotoxic or clastogenic substance (Umar-Tsafe et al., 2004). Recent studies reveal that ROS acts both as an upstream signal that triggers TP53 activation and as a downstream factor that mediates apoptosis (Liu et al., 2008). Accordingly, GTN treatment of SK-Hep1 cells for 24 h somewhat induced an extended stress response and irreparable damage, followed by the transactivation of TP53-dependent prooxidant genes for the removal of mutated cells via apoptosis. In contrast, GTN triggered DNA damage-induced ROS formation and delayed the apoptotic process in TP53-negative Hep-3B cells (with a higher IC_{50} than that for TP53-positive SK-Hep1 cells), similar to that observed in the epidermis of *TP53*-knockout mice (Ikehata et al., 2010).

In conclusion, GTN induces cytotoxicity, ROS accumulation, DNA double-strand breaks, and mitochondria- and CASP-mediated apoptosis in both TP53-positive SK-Hep1 and TP53-negative Hep-3B cells. Both the TP53 and PMAIP1 proteins were translocated into the mitochondria, where they triggered CYCS release and apoptosis after GTN treatment. Transactivation of *PMAIP1* by pTP53(Ser15) protein after GTN treatment or by transcription factor(s) other rather than TP53, E2F1, MYC, TP63 or TP73 might play a crucial role in GTN-induced apoptosis in HCC-derived cells.

Supplementary materials related to this article can be found online at doi:10.1016/j.taap.2011.07.002.

Conflict of interest

The authors declare that there are no conflicts of interest.

Acknowledgments

The authors gratefully acknowledge Dr. Shu-Chun Teng (National Taiwan University, Taipei, Taiwan) and Ming-Hong Tai (National Sun Yat-sen University, Kaohsiung, Taiwan) for valuable discussions; and the finial support provided by the National Science Council (NSC, grant number 96-2320-B-110-007) to YL Shiue.

References

Adams, J.M., Cory, S., 2007. The Bcl-2 apoptotic switch in cancer development and therapy. Oncogene 26, 1324–1337.
Bressac, B., Galvin, K.M., Liang, T.J., Isselbacher, K.J., Wands, J.R., Ozturk, M., 1990. Abnormal structure and expression of p53 gene in human hepatocellular carcinoma. Proc. Natl. Acad. Sci. U. S. A. 87, 1973–1977.
Chen, W.Y., Wu, C.C., Lan, Y.H., Chang, F.R., Teng, C.M., Wu, Y.C., 2005. Goniothalamin induces cell cycle-specific apoptosis by modulating the redox status in MDA-MB-231 cells. Eur. J. Pharmacol. 522, 20–29.
D'Amours, D., Sallmann, F.R., Dixit, V.M., Poirier, G.G., 2001. Gain-of-function of poly (ADP-ribose) polymerase-1 upon cleavage by apoptotic proteases: implications for apoptosis. J. Cell Sci. 114, 3771–3778.
Fabregat, I., 2009. Dysregulation of apoptosis in hepatocellular carcinoma cells. World J. Gastroenterol. 15, 513–520.
Fatima, A., Kohn, L.K., Carvalho, J.E., Pilli, R.A., 2006. Cytotoxic activity of (S)-goniothalamin and analogues against human cancer cells. Bioorg. Med. Chem. 14, 622–631.
Ghiotto, F., Fais, F., Bruno, S., 2010. BH3-only proteins: the death-puppeteer's wires. Cytometry A 77, 11–21.
Hallaert, D.Y., Spijker, R., Jak, M., Derks, I.A., Alves, N.L., Wensveen, F.M., de Boer, J.P., de Jong, D., Green, S.R., van Oers, M.H., Eldering, E., 2007. Crosstalk among Bcl-2 family members in B-CLL: seliciclib acts via the Mcl-1/Noxa axis and gradual exhaustion of Bcl-2 protection. Cell Death Differ. 14, 1958–1967.
Hershko, T., Ginsberg, D., 2004. Up-regulation of Bcl-2 homology 3 (BH3)-only proteins by E2F1 mediates apoptosis. J. Biol. Chem. 279, 8627–8634.
Hoshida, Y., Toffanin, S., Lachenmayer, A., Villanueva, A., Minguez, B., Llovet, J.M., 2010. Molecular classification and novel targets in hepatocellular carcinoma: recent advancements. Semin. Liver Dis. 30, 35–51.
Ikehata, H., Okuyama, R., Ogawa, E., Nakamura, S., Usami, A., Mori, T., Tanaka, K., Aiba, S., Ono, T., 2010. Influences of p53 deficiency on the apoptotic response, DNA damage removal and mutagenesis in UVB-exposed mouse skin. Mutagenesis 25, 397–405.
Inayat-Hussain, S.H., Osman, A.B., Din, L.B., Ali, A.M., Snowden, R.T., MacFarlane, M., Cain, K., 1999. Caspases-3 and -7 are activated in goniothalamin-induced apoptosis in human Jurkat T-cells. FEBS Lett. 456, 379–383.
Inayat-Hussain, S.H., Annuar, B.O., Din, L.B., Ali, A.M., Ross, D., 2003. Loss of mitochondrial transmembrane potential and caspase-9 activation during apoptosis induced by the novel styryl-lactone goniothalamin in HL-60 leukemia cells. Toxicol. In Vitro 17, 433–439.
Inayat-Hussain, S.H., Chan, K.M., Rajab, N.F., Din, L.B., Chow, S.C., Kizilors, A., Farzaneh, F., Williams, G.T., 2010. Goniothalamin-induced oxidative stress, DNA damage and apoptosis via caspase-2 independent and Bcl-2 independent pathways in Jurkat T-cells. Toxicol. Lett. 193, 108–114.
Inoue, S., Riley, J., Gant, T.W., Dyer, M.J., Cohen, G.M., 2007. Apoptosis induced by histone deacetylase inhibitors in leukemic cells is mediated by Bim and Noxa. Leukemia 21, 1773–1782.
Kaghad, M., Bonnet, H., Yang, A., Creancier, L., Biscan, J.C., Valent, A., Minty, A., Chalon, P., Lelias, J.M., Dumont, X., Ferrara, P., McKeon, F., Caput, D., 1997. Monoallelically expressed gene related to p53 at 1p36, a region frequently deleted in neuroblastoma and other human cancers. Cell 90, 809–819.
Kuerbitz, S.J., Plunkett, B.S., Walsh, W.V., Kastan, M.B., 1992. Wild-type p53 is a cell cycle checkpoint determinant following irradiation. Proc. Natl. Acad. Sci. U. S. A. 89, 7491–7495.
Kulesz-Martin, M., Lagowski, J., Fei, S., Pelz, C., Sears, R., Powell, M.B., Halaban, R., Johnson, J., 2005. Melanocyte and keratinocyte carcinogenesis: p53 family protein activities and intersecting mRNA expression profiles. J. Investig. Dermatol. Symp. Proc. 10, 142–152.
Kurata, K., Yanagisawa, R., Ohira, M., Kitagawa, M., Nakagawara, A., Kamijo, T., 2008. Stress via p53 pathway causes apoptosis by mitochondrial Noxa upregulation in doxorubicin-treated neuroblastoma cells. Oncogene 27, 741–754.
Lan, Y.H., Chang, F.R., Yu, J.H., Yang, Y.L., Chang, Y.L., Lee, S.J., Wu, Y.C., 2003. Cytotoxic styrylpyrones from *Goniothalamus amuyon*. J. Nat. Prod. 66, 487–490.
Lan, Y.H., Chang, F.R., Liaw, C.C., Wu, C.C., Chiang, M.Y., Wu, Y.C., 2005. Digoniodiol, deoxygoniopypyrone A, and goniofupyrone A: three new styryllactones from *Goniothalamus amuyon*. Planta Med. 71, 153–159.
Lan, Y.H., Chang, F.R., Yang, Y.L., Wu, Y.C., 2006. New constituents from stems of *Goniothalamus amuyon*. Chem. Pharm. Bull. (Tokyo) 54, 1040–1043.
Liu, B., Chen, Y., St Clair, D.K., 2008. ROS and p53: a versatile partnership. Free Radic. Biol. Med. 44, 1529–1535.
Livingstone, L.R., White, A., Sprouse, J., Livanos, E., Jacks, T., Tlsty, T.D., 1992. Altered cell cycle arrest and gene amplification potential accompany loss of wild-type p53. Cell 70, 923–935.
Marchenko, N.D., Zaika, A., Moll, U.M., 2000. Death signal-induced localization of p53 protein to mitochondria. A potential role in apoptotic signaling. J. Biol. Chem. 275, 16202–16212.
Mereyala, H.B., Joe, M., 2001. Cytotoxic activity of styryl lactones and their derivatives. Curr. Med. Chem. Anticancer Agents 1, 293–300.
Moll, U.M., Zaika, A., 2001. Nuclear and mitochondrial apoptotic pathways of p53. FEBS Lett. 493, 65–69.
Moll, U.M., Wolff, S., Speidel, D., Deppert, W., 2005. Transcription-independent pro-apoptotic functions of p53. Curr. Opin. Cell Biol. 17, 631–636.
Murphy, P.J., Galigniana, M.D., Morishima, Y., Harrell, J.M., Kwok, R.P., Ljungman, M., Pratt, W.B., 2004. Pifithrin-alpha inhibits p53 signaling after interaction of the tumor suppressor protein with hsp90 and its nuclear translocation. J. Biol. Chem. 279, 30195–30201.
Narayanan, P.K., Ragheb, K., Lawler, G., Robinson, J.P., 1997. Defects in intracellular oxidative metabolism of neutrophils undergoing apoptosis. J. Leukoc. Biol. 61, 481–488.
Nikiforov, M.A., Riblett, M., Tang, W.H., Gratchouck, V., Zhuang, D., Fernandez, Y., Verhaegen, M., Varambally, S., Chinnaiyan, A.M., Jakubowiak, A.J., Soengas, M.S., 2007. Tumor cell-selective regulation of NOXA by c-MYC in response to proteasome inhibition. Proc. Natl. Acad. Sci. U. S. A. 104, 19488–19493.
Nowak, A.K., Chow, P.K., Findlay, M., 2004. Systemic therapy for advanced hepatocellular carcinoma: a review. Eur. J. Cancer 40, 1474–1484.
Oda, E., Ohki, R., Murasawa, H., Nemoto, J., Shibue, T., Yamashita, T., Tokino, T., Taniguchi, T., Tanaka, N., 2000. Noxa, a BH3-only member of the Bcl-2 family and candidate mediator of p53-induced apoptosis. Science 288, 1053–1058.
Offer, H., Erez, N., Zurer, I., Tang, X., Milyavsky, M., Goldfinger, N., Rotter, V., 2002. The onset of p53-dependent DNA repair or apoptosis is determined by the level of accumulated damaged DNA. Carcinogenesis 23, 1025–1032.
Ploner, C., Kofler, R., Villunger, A., 2008. Noxa: at the tip of the balance between life and death. Oncogene 27 (Suppl 1), S84–S92.
Shibue, T., Takeda, K., Oda, E., Tanaka, H., Murasawa, H., Takaoka, A., Morishita, Y., Akira, S., Taniguchi, T., Tanaka, N., 2003. Integral role of Noxa in p53-mediated apoptotic response. Genes Dev. 17, 2233–2238.
Shiue, Y.L., Chen, L.R., Chen, C.F., Chen, Y.L., Ju, J.P., Chao, C.H., Lin, Y.P., Kuo, Y.M., Tang, P.C., Lee, Y.P., 2006. Identification of transcripts related to high egg production in the chicken hypothalamus and pituitary gland. Theriogenology 66, 1274–1283.

Speidel, D., 2010. Transcription-independent p53 apoptosis: an alternative route to death. Trends Cell Biol. 20, 14–24.
Staib, F., Hussain, S.P., Hofseth, L.J., Wang, X.W., Harris, C.C., 2003. TP53 and liver carcinogenesis. Hum. Mutat. 21, 201–216.
Steele, A.J., Prentice, A.G., Hoffbrand, A.V., Yogashangary, B.C., Hart, S.M., Lowdell, M.W., Samuel, E.R., North, J.M., Nacheva, E.P., Chanalaris, A., Kottaridis, P., Cwynarski, K., Wickremasinghe, R.G., 2009. 2-Phenylacetylenesulfonamide (PAS) induces p53-independent apoptotic killing of B-chronic lymphocytic leukemia (CLL) cells. Blood 114, 1217–1225.
Tice, R.R., Agurell, E., Anderson, D., Burlinson, B., Hartmann, A., Kobayashi, H., Miyamae, Y., Rojas, E., Ryu, J.C., Sasaki, Y.F., 2000. Single cell gel/comet assay: guidelines for in vitro and in vivo genetic toxicology testing. Environ. Mol. Mutagen. 35, 206–221.
Umar-Tsafe, N., Mohamed-Said, M.S., Rosli, R., Din, L.B., Lai, L.C., 2004. Genotoxicity of goniothalamin in CHO cell line. Mutat. Res. 562, 91–102.
Watson, J.L., Hill, R., Yaffe, P.B., Greenshields, A., Walsh, M., Lee, P.W., Giacomantonio, C.A., Hoskin, D.W., 2010. Curcumin causes superoxide anion production and p53-independent apoptosis in human colon cancer cells. Cancer Lett. 297, 1–8.
Worns, M.A., Weinmann, A., Schuchmann, M., Galle, P.R., 2009. Systemic therapies in hepatocellular carcinoma. Dig. Dis. 27, 175–188.
Wu, Y.C., Duh, C.Y., Chang, F.R., Chang, G.Y., Wang, S.K., Chang, J.J., McPhail, D.R., McPhail, A.T., Lee, K.H., 1991. The crystal structure and cytotoxicity of goniodiol-7-monoacetate from *Goniothalamus amuyon*. J. Nat. Prod. 54, 1077–1081.
Xiao, A., Li, H., Shechter, D., Ahn, S.H., Fabrizio, L.A., Erdjument-Bromage, H., Ishibe-Murakami, S., Wang, B., Tempst, P., Hofmann, K., Patel, D.J., Elledge, S.J., Allis, C.D., 2009. WSTF regulates the H2A.X DNA damage response via a novel tyrosine kinase activity. Nature 457, 57–62.
Yang, A., Kaghad, M., Wang, Y., Gillett, E., Fleming, M.D., Dotsch, V., Andrews, N.C., Caput, D., McKeon, F., 1998. p63, a p53 homolog at 3q27-29, encodes multiple products with transactivating, death-inducing, and dominant-negative activities. Mol. Cell 2, 305–316.
Yu, J., Zhang, L., 2005. The transcriptional targets of p53 in apoptosis control. Biochem. Biophys. Res. Commun. 331, 851–858.
Zhou, F.S., Tang, W.D., Mu, Q., Yang, G.X., Wang, Y., Liang, G.L., Lou, L.G., 2005. Semisynthesis and antitumor activities of new styryl-lactone derivatives. Chem Pharm Bull (Tokyo) 53, 1387–1391.